2013-03-15

Evidences for Protein-Protein Interactions Between PstB and PhoU in the Phosphate Signaling Complex of Escherichia coli

Kristine Dawn Johns
Brigham Young University - Provo

Evidences for Protein-Protein Interactions Between PstB and PhoU in the Phosphate Signaling Complex of *Escherichia coli*

Kristine D. Johns

A thesis submitted to the faculty of
Brigham Young University
in partial fulfillment of the requirements for the degree of

Master of Science

William R. McCleary, Chair
Joel S. Griffitts
Julianne H. Grose

Department of Microbiology and Molecular Biology

Brigham Young University

March 2013

ABSTRACT

Evidences for Protein-Protein Interactions Between PstB and PhoU in the Phosphate Signaling Complex of *Escherichia coli*

Kristine D. Johns
Department of Microbiology and Molecular Biology, BYU
Master of Science

The $PstSCAB_2$ complex serves the dual function of being a phosphate transporter as well as the primary sensor of phosphate for the Pho regulon. PhoU is an integral protein required for the signal from $PstSCAB_2$ to be transmitted to PhoR. Our hypothesis is that conformational changes of $PstSCAB_2$ during the phosphate transport process are the mechanism by which information about environmental phosphate levels are transduced to the cell. Additionally, we propose that direct protein-protein interactions between PhoU and the alternating conformations of $PstSCAB_2$ mediate PhoU interactions with PhoR. By means of genetic and biochemical approaches, we have found substantial evidence supporting both these hypotheses.

Keywords: Pho regulon, two-component, ABC transporter, PstB, PhoU

TABLE OF CONTENTS

LIST OF TABLES

LIST OF FIGURES

INTRODUCTION

To survive varying environmental conditions, bacteria must be able to sense environmental stimuli and relay signals to the cell to adapt to current conditions. Gene regulation is a key mechanism of adaptation, and many organisms employ the use of two- component signaling (TCS) pathways to regulate the expression of adaptive genes. In turn, up-regulation of target genes coding for proteins, such as membrane transporters that can be used to bring substrates into the cell or enzymes that can be employed for metabolic purposes. These specific mechanisms are the subject of interest in understanding how bacteria, such as *Escherichia coli,* maintain homeostatic balance in varying phosphate environmental conditions.

The phosphate regulatory system in *Escherichia coli*, known as the Pho regulon, utilizes a TCS pathway to control phosphate levels within the cell. The partner proteins in this TCS, PhoR and PhoB, regulate target Pho genes which, when expressed, allow the cell to employ alternate sources of phosphate. One of the operons under the regulation of PhoR-PhoB encodes for an ATP-binding cassette (ABC) transporter $PstSCAB_2$. This transporter is used to import inorganic phosphate (P_i) into the cell in low phosphate conditions (~4uM) (2, 3). Interestingly, expression of $PstSCAB_2$, as well as an accessory protein, PhoU, is necessary for phosphate signal transduction to PhoR (4, 5).

The purpose of this introduction is to provide a foundational review of the role TCSs and ABC transporters play in cell adaptation, in order to better understand the Pho regulon of *E. coli*. To do this, we will begin by reviewing the general structure and function of TCSs and ABC transporters in bacteria. We will then overview the Pho regulon system in *E. coli*, specifically describing the structure and function of PhoR-PhoB and $PstSCAB_2$. Finally, we will

discuss the interactive nature of $PstSCAB_2$, PhoR-PhoB, and PhoU in regulating gene expression in the Pho regulon of *E. coli*.

Two-component signaling

Two-component signal (TCS) transduction is one of the most abundant multistep signaling pathways used by bacteria to accomplish the task of connecting changes in the environment with adaptive responses in the cell (6, 7). These pathways regulate important cellular processes ranging from cell development and virulence, to motility and metabolism, with many species expressing over twenty to thirty different TCSs (8). TCSs represent a large family of energy-dependent signal transducers, the most basic of which consist of two partner proteins, a histidine kinase and a response regulator. However, many organisms have evolved pathways involving complex cascades of proteins (9). For the purposes of this paper, we will focus on the simple two-partner system of bacterial two-component signaling.

The defining feature of signaling pathways is the interplay of phosphorylating and dephosphorylating proteins to control the signal being transduced. TCS proteins rely on a phosphotransfer between the histidine kinase (the phosphor-donor) and the response regulator (the phospho-acceptor). Both proteins contain highly conserved domains required for successful regulation of signal transduction. A brief overview of the details of these partner proteins will prove helpful in better understanding the PhoR-PhoB TCS in *E. coli.*

Histidine Kinases

In bacteria, most HKs are membrane receptors that contain an extracellular domain required to fix the protein to the membrane and sense substrate, and a cytoplasmic domain responsible for transducing the sensory signal to the response regulator. For gram-negative

bacteria such as *E. coli,* the extracellular domain is more accurately described as the periplasmic domain.

Extracellular domain

Primarily located at the N-terminus of the protein, the extracellular domain typically contains alpha helical structures used to span the membrane and connect to a sensory domain located on the external side of the membrane (10). The majority of HKs have a sensory domain included with the transmembrane domain, allowing the protein to directly sense environmental stimuli (11) . The specificity of each domain varies: some have low-affinity and as such could have the ability to sense a spectrum of stimuli, typically at higher concentrations; others have high- affinity for a specific substrate of interest recognized even at very low concentrations (12). The types of stimuli sensed by these proteins include, but are not limited to, receptor molecules, cell envelope pressure and stress, electrochemical gradients and light (8, 13, 14). Related sensory domains typically share common secondary and tertiary structures; however, most extracellular domains do not share similar primary sequence structure (8).

Though the amino acid sequences vary greatly in HK sensory domains, the commonalities between their final structure and function make it possible for researchers to categorize them into three general groups. First, and the largest of the groups, are the HKs that contain an extracellular sensory domain flanked by two transmembrane helices. This format allows the HK versatility in its methods of sensing stimuli (10). The second topology forms HKs with no extracellular domain. These HKs structurally consist of few alpha-helices used solely for membrane localization, and require a substrate-binding protein to receive their source of stimuli (8) This class of HKs are the focus of this paper. The final group of HKs uses a cytoplasmic-

faced sensory domain to sense and regulate diffused materials from within the cell (15). It is important to note that many HKs combine several characteristics of each category, thus making the true distinctions far less concrete. Regardless of what category they may fall into, once the HK protein senses a signal, its kinase activity is regulated.

Cytoplasmic domain

The cytoplasmic domain of the HK is the region responsible for its kinase function. The catalytic (CA) domain and DHp domain, found in the cytosolic core of the protein, are the two universal features found in all HKs (16, 17). The CA domain is a highly conserved motif primarily located at the C-terminus of the protein (14, 18, 19). This domain is responsible for binding ATP and catalyzing autophosphorylation of a key histidine residue located in the DHp domain (7). The DHp domain is the interactive site for dimerization that houses the key histidine residue required for phosphorylation (7, 19). Some classes of these HK domains can exhibit multiple enzymatic activities, such as response regulator phosphatase or autokinase functions (20, 21). It is important to note that while all HKs have kinase capabilites, not all are able to exhibit multiple enzymatic functions. For those HKs that do have this ability, conformational changes in the two cytoplasmic domains (CA and DHp) are necessary for the HK to alternate between these different enzymatic states (21). How this process works remains unclear. However, in general, when the interface between the two domains is altered, phosphorylation is prevented and the HK remains inactive or, in some instances, behaves as a phosphatase. It is these conformational changes that make the two-component signaling system capable of regulating signal transduction.

Response Regulators

The primary function of response regulators (RR) is to receive stimulus messages from the HK and then affect cellular regulatory responses. RRs belong to a vast superfamily that share a highly conserved domain known as the receiver, or REC, domain (22). The REC domain, located on the N-terminus, is linked to an effector domain, a less-conserved structure used to affect cellular responses typically as a transcription factor (23). The variation of the effector domain is vital, as each response regulator must have an effector domain specific to the response it is regulating. A response regulator uses these domains to fulfill three main responsibilities: first, it interacts with the HK for phospho-transfer; second, it catalyzes dephosphorylation; finally, it regulates the effector domain according to its phosphorylation state (24, 25) The interaction and structure of these domains play a vital role in controlling cellular responses.

REC domain

The key function of the REC domain is to catalyze phosphate transfer from the HK to the RR (25, 26). Transfer takes place by donating the phosphate bound to the histidine in the HK's DHp domain onto a conserved aspartate residue located in the REC domain of the RR. According to Pfam analysis, a fourth of the REC domain sequence identity is related, with a few key amino acid residues that are highly conserved between the families (9). These conserved sites are necessary for the REC domain to respond as a phosphorylation-activated switch (27). Phosphorylation of RR's REC domain activates the protein by altering its conformation, allowing the effector domain to mediate gene expression or repression (28-31). Without phosphorylation of the REC domain, the response regulator will remain in an inactive state.

Deactivation of the RR requires removal of the added phosphate by a phosphatase, or autodephosphorylation (32, 33).

Effector domain

Once activated, the response regulator induces an output response through the interactive effector domain (23). The majority of response regulators are transcription factors, having an effector domain with specificity to bind to promoter and regulatory factors upstream target gene sequences (23, 34, 35). Given the sheer number of regulated genes within a cell, maintaining the delicate balance between activation and inhibition would require RRs to have effector domains containing unique specificity for the output response it regulates. For this reason the effector domain has the greatest amount of variation of all the interactive domains in the TCS pathway. However, although these effector domains vary greatly, they still serve a similar purpose: to regulate cellular responses for the benefit of the cell.

A large majority of response regulators act as transcription factors for target genes. Typically, transcription factor binding will require the response regulator to dimerize before it is able to recognize and bind to the upstream sequence (22, 36-38). Some classes of RR will act as transcription inhibitors, halting or preventing the expression of specific genes. However, the majority of RRs are transcription activators, inducing the expression of proteins and enzymes needed for survival (39). For the Pho regulon of *E. coli,* PhoB-induced expression of target genes coding for the ABC transporter $PstSCAB_2$ is vital for signal transduction and cell survival (40).

ABC Transporters

ATP-binding cassette (ABC) transporters are members of one of the largest and oldest protein families, and are a class of molecular complexes used to pump substrate across biological membranes through the use of ATP hydrolysis (41). They are found in practically every organism including bacteria, fungi, plants, animals, and humans (42) and are involved in the development of multi-drug resistance as well as genetic diseases such as cystic fibrosis (43-45). As such, they merit the need for significant research. The name is derived from the complex's ATP-binding cassette responsible for energy production and substrate transfer. These membrane transporters obtain energy through ATP hydrolysis in order to facilitate the transport of substrate into the cell (46, 47). Types of substrate carried by these transporters include lipids, metabolic products, and pharmaceutical drugs. ABC transporters are separated into two primary classes, importers and exporters, though for the purposes of this paper, we will focus on bacterial ABC importers.

Bacterial ABC importers are responsible for sensing and importing substrate into the cell. Substrate importation involves two key aspects: substrate recognition facilitated by a substrate-binding protein (periplasmic for gram negative bacteria, extracellular for gram positive bacteria), and conformational changes of the structural components of the ABC transporter coupled to ATP binding and hydrolysis (41, 48). The structural components of the transporter are comprised of a few key proteins or domains: two transmembrane polypeptides that form the transmembrane domain (TMD), a dimer of cytosolic peripheral proteins referred to as the nucleotide-binding domain (NBD), and a periplasmic or extracellular binding protein.

Transmembrane domain

Substrate recognition requires a peripheral protein exhibiting a high affinity for the substrate of interest and an interactive domain that allows it to associate closely with the TMD to facilitate substrate transport (41, 48). The TMD's primary responsibility is substrate recognition followed by a conformational change to channel passage of the substrate into the cell. Typically, both transmembrane domains are comprised of six α-helices used to span the membrane, making a total of twelve membrane-spanning helices for the entire transporter (49, 50). These membrane spanning domains have highly conserved architectural features found in many other families of transporters (42). In spite of the fact that they share such similarity with other families of transporters, ABC transporter TMDs are classified separately because of their ability to bind the nucleotide-binding domain (NBD), a protein dimer responsible for ATP hydrolysis. The ATPase activity of the NBD is the defining feature that characterizes this superfamily (51).

Nucleotide-binding domain

The nucleotide-binding domain is a protein dimer responsible for binding and hydrolyzing ATP in order to catalyze substrate transport. The dimer associates with the TMD on the cytosolic side of the membrane and consists of two separate domains that coordinate ATPase activity (52-54). The NBD contains several highly conserved structural motifs necessary for its function. Three of these required conserved residues are the Walker A motif, the Walker B motif, and the ABC signature motif (54). The Walker A motif is the site necessary for binding ATP. The conserved amino acid residues form a loop that holds onto the beta and gamma phosphates of ATP. The Walker B motif, on the other hand, is the domain responsible for ATP hydrolysis (48, 51, 55). The ABC signature motif serves the purpose of stabilizing the bound

ATP in the sister dimer (56). The collaborative interactions of these motifs are the mechanisms believed to drive the transporter into its alternative conformations (48, 49, 51, 55).

Conformational changes

Substrate transport for ABC transporters requires coupling ATP hydrolysis to a corresponding conformational change in the complex, allowing substrate to cross the biological membrane (50, 57). A current model, explaining the related conformational changes between the TMD and NBD, proposes that the transporter alternates between two conformational states: a conformation open to the cytoplasm (active-state) and a closed (resting-state) conformation (58, 59). For example, Daus *et al.* discovered that when mutations were made in the Walker B motif of NBD dimer, MalK, the $MalFGK_2$ transporter (a maltose ABC transporter) locked in an open, active conformation (59). Conversely, when mutations were made in the ABC signature motif of MalK, the transporter remained in a closed, resting state (56, 59). These findings provide insights in better understanding the interactive nature of $PstSCAB_2$ in phosphate signal transduction for the Pho regulon.

The Pho Regulon

Phosphate signal transduction in *Escherichia coli* is an inhibitory pathway that signals for the repression of otherwise constitutively expressed Pho genes. As mentioned earlier, Pho regulon signal transduction is dependent on a combination of proteins and protein complexes. Two of these proteins, PhoR and PhoB, comprise a TCS responsible for regulating target genes of the Pho Regulon (60). Another protein complex necessary for phosphate signal transduction is the ABC transporter, $PstSCAB_2$, without which phosphate genes remain constitutively expressed. A final protein necessary for signal transduction is PhoU—an accessory peripheral

membrane protein, with unknown function, required for successful signaling (61). A signaling complex involving an interaction of these proteins has been proposed but never demonstrated (see Fig. 1) (4).

The two-component system, PhoR-PhoB

The TCS proteins PhoR and PhoB control expression of Pho regulon genes. The sensory histidine kinase, PhoR, is responsible for receiving the signal regarding environmental phosphate levels and passing the signal onto PhoB, a DNA-binding response regulator. PhoB is a transcription activator that, when activated, induces expression of Pho genes. Without an external signal, the default state of PhoR is as a kinase, phorphorylating PhoB and, in turn, constitutively expressing Pho genes (40, 62).

PhoB – Response Regulator (RR)

A large number of genes are regulated by the Pho regulon through the response regulator PhoB. Environmental phosphate levels determine gene expression (4, 62-64). In high phosphate conditions, these genes are repressed to conserve cell resources and energy. However, in low phosphate conditions, these genes are expressed in order to utilize alternative phosphate sources necessary for the cell (65). PhoB is the transcription factor responsible for regulating expression of these genes.

Structurally, PhoB contains two key domains: a REC domain, responsible for receiving signal (via phospho-transfer) from PhoR, and the DNA-binding domain, an effector domain with specificity for an upstream regulatory element of Pho genes, called the PhoBox (66, 67). PhoB is activated by phosphorylation and deactivated with removal of the phosphate by a phosphatase or autodephosphorylation (38). Phosphorylation takes place in the REC domain on a highly

conserved aspartate residue. In its active state, PhoB is a transcription activator that dimerizes in order to bind the PhoBox and actively recruits RNA polymerase to upregulate expression of a variety of phosphate genes (68-70). These Pho genes include *phoR* and *phoB* of the TCS; the ABC transporter, *pstSCAB*$_2$, and *phoU*; and genes such as *phoA* that codes for the enzyme alkaline phosphatase, a key enzyme used for measuring activation of the Pho Regulon (4, 69).

PhoR – Sensory Histidine Kinase (HK)

PhoR is responsible for activating and deactivating PhoB. As explained, PhoR acts as a dimer and plays a dual role of kinase and phosphatase. In its natural state, PhoR autophosphorylates and behave as a kinase (71). In its kinase role, PhoR is a phospho-donor to PhoB, transferring a phosphate from its DHp domain to an aspartate residue in the REC domain of PhoB (71). However, if PhoR is prevented from auto-phosphorylating, it loses the capacity of donating phosphate to PhoB, and may then function as a phosphatase, removing phosphate from PhoB rendering it inactive (20).

PhoR contains several highly conserved domains necessary for its function. It has a catalytic domain, responsible for hydrolyzing ATP for autophorphorylation, and a DHp domain, the interactive site for dimerization that contains the conserved histidine residue needed for phosphorylation (40, 66). It also contains a PAS domain that may be a potential interactive site for receiving the phosphate signal (66, 71). Additionally, PhoR contains an N-terminal transmembrane domain responsible for membrane localization. However, the transmembrane portion lacks a sensory domain, implying that PhoR is unable to receive a direct signal and must instead receive the signal indirectly, perhaps from PstSCAB$_2$, PhoU, or both (66). Some specific questions arise from this model. How does PhoR receive the signal that determines whether it

acts as a kinase or a phosphatase? Since $PstSCAB_2$ is required for phosphate signaling, does this imply a direct protein-protein interaction between the ABC transporter and PhoR in order to transduce the signal?

The ABC transporter, $PstSCAB_2$

$PstSCAB_2$ is a high-affinity, low-velocity ABC transporter responsible for importing inorganic phosphate (P_i) from the periplasm into the cell. In low phosphate conditions $PstSCAB_2$ is highly expressed; in high phosphate environments, it is expressed but minimally. Transport of P_i in high phosphate conditions rests primarily on the secondary transporters, PitA and PitB (4, 64). The genes that code for $PstSCAB_2$ are all located on the same operon, along with PhoU, and are regulated by PhoB (69). Much remains to be discovered about this transporter, as most structural and functional aspects of $PstSCAB_2$ are based on the highly studied maltose transporter, $MalFGK_2$ (a homolog of $PstSCAB_2$). However, one thing is known: expression of $PstSCAB_2$ is required for phosphate signal transduction as mutations in any of the component genes will inhibit signaling (4).

TMD- PstA and PstC

Based on crystal structures of the $MalFGK_2$ TMD proteins, MalF and MalG, it is assumed that PstA and PstC also form a heterodimeric complex than spans the membrane and creates a channel for phosphate transport (56). Transport requires the periplasmic sensory protein, PstS, to bind P_i and present it to the transporter (50). When phosphate-bound PstS associates tightly with the two transmembrane proteins, they are proposed to undergo a conformational change opening the transporter and allowing phosphate to enter the cell (41). How the transition between open and closed conformations of $PstSCAB_2$ is accomplished has yet

to be determined. Currently it is assumed that ATP hydrolysis by the PstB dimer is the motor by which conformational changes are driven (57, 72, 73) .

NBD- PstB dimer

Activation of phosphate transport requires energy provided by the NBD dimer, PstB. The dimer provides this energy by binding and hydrolyzing ATP. The coupling of this ATPase activity to conformational changes in the transporter is the assumed mechanism by which $PstSCAB_2$ alternates between open and closed conformations. An active transition from closed to open conformations allows phosphate to be brought into the cell. Following transport, the complex returns to a closed, resting state. Evidence for this hypothesis comes from research done on the homolog $MalFGK_2$ maltose transporter, where mutations made to the Walker B and ABC signature motifs of MalK locked the transporter in closed and open conformations, respectively. A BLAST alignment of MalK and PstB shows that PstB also contains the highly conserved Walker A, Walker B, and ABC Signature motifs. By making similar mutations to PstB, it is assumed that $PstSCAB_2$ will similarly lock in open and closed conformations. Should this assumption be correct, it raises a few questions. First, by alternating between these open and closed conformations, is $PstSCAB_2$ able to sense environmental phosphate conditions? And second, if this is the case, how is the signal then transduced to PhoR?

PhoU involvement in signal transduction

Vital in this signaling pathway is the peripheral membrane protein, PhoU. The role of PhoU in signal transduction is unknown; however, it is assumed to act as an accessory protein that interacts at the membrane aiding communication between $PstSCAB_2$ and PhoR-PhoB (4, 40, 74). Hsieh and Wanner's model of the Pho regulon suggests that the PstB dimer of $PstSCAB_2$ is

the key protein used in relaying the phosphate signal onto PhoR (4). For this to occur, signal transduction could involve a direct interaction between PstB and PhoR, or it could require the signal to be passed through the intermediate protein, PhoU (75). Another possibility could involve the formation of an inhibitory complex involving all three proteins: PstB, PhoU and PhoR (4). As of yet, none of these interactions have been demonstrated. The purpose of this research is to identify potential protein-protein interactions between PstB and PhoU and to determine if conformation changes in $PstSCAB_2$ affect these interactions.

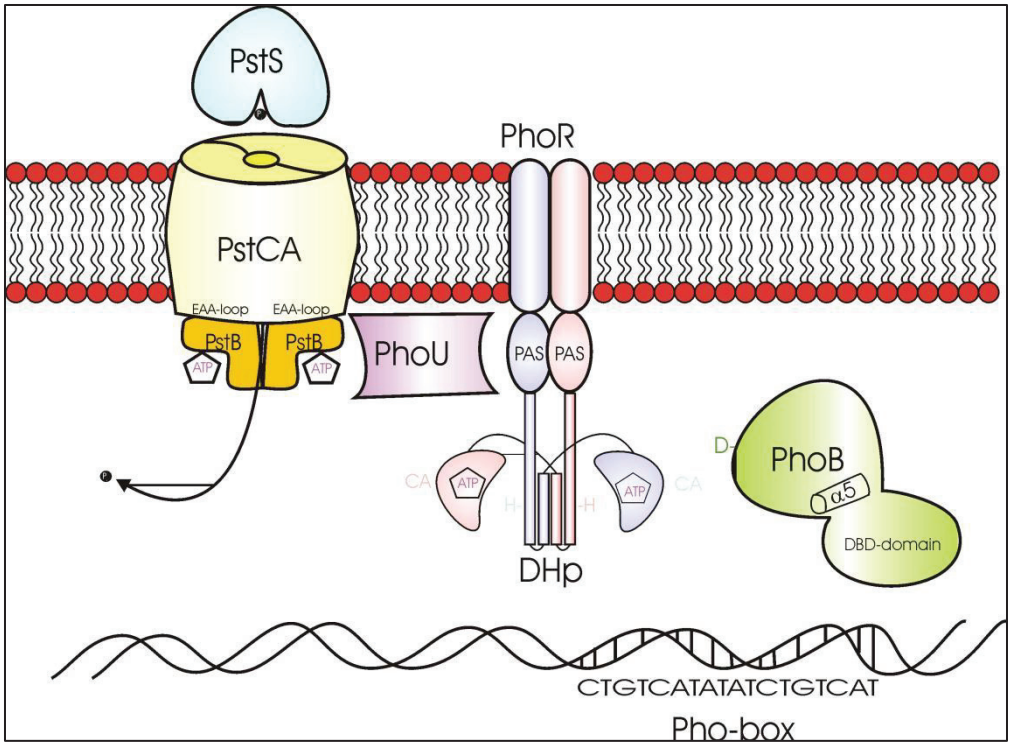

Figure 1: Overview of the Pho regulon

The major components of the Pho regulon consist of the two-component signaling (TCS) proteins, PhoR and PhoB, an ABC transporter, $PstSCAB_2$, and the accessory protein, PhoU. The phosphate signal is a negative regulator of Pho gene expression. PhoR behaves as a kinase in its natural state, continually phosphorylating PhoB and inducing target gene expression. The phosphate signal triggers for the repression of these Pho genes by activating the phosphatase function of PhoR. Signal transduction depends on the presence of $PstSCAB_2$ and PhoU. A model involving a signaling complex of $PstSCAB_2$, PhoU, and PhoR is the proposed mechanism for signal transduction.

MATERIALS AND METHODS

Media and growth conditions

Cultures were grown in LB, MOPS low phosphate, and MOPS high phosphate minimal media (76). LB broth contained the following: 1% Bacto-tryptone, 0.5% yeast extract, and 1% NaCl in ddH_2O, and was sterilized by autoclaving. SOC medium contained the following: 2% Tryptone, 0.5% yeast extract, 8.6 mM concentration of NaCl, 2.5 mM concentration of KCl, 20 mM concentration of $MgSO_4$, and 20 mM glucose, and was also sterilized by autoclaving.

Low phosphate MOPS medium was prepared using a 1 X concentration of MOPS Mixture (Teknova) with 0.4% glucose (20% stock solution) and 0.1 mM K_2HPO_4 (132mM stock solution). High phosphate MOPS medium was prepared using a 1 X concentration of MOPS Mixture Mixture, 0.06% glucose (20% stock solution), and 2mM K_2HPO_4 (132 mM stock solution). MOPS no phosphate medium was prepared using the same concentrations as the low phosphate MOPS medium except no K_2HPO_4 was added. All MOPS media were sterilized by filtration. The antibiotics ampicillin (100 μg/ml) and kanamycin (50 μg/ml) were used for strain selection. Plasmid expression was induced using varying concentrations of isopropyl β-D-1-thiogalactopyranoside (IPTG).

Plates for culturing bacteria were comprised of LB agar (1 L LB broth solidified with 14 g bacto-agar) containing ampicillin (100 μg/ml) and/or kanamycin (50 μg/ml) when appropriate. LB/X-gal plates for two-hybrid screens were made of LB agar containing X-gal (40 μg/ml) and IPTG (500 μM), as well as both ampicillin (100 μg/ml) and kanamycin (50 μg/ml). MacConkey/maltose plates for two-hybrid screens were made by dissolving 40 g of MacConkey agar into 1 L of distilled water. Maltose was added to the autoclaved solution at 1%

concentration (20% stock solution of glucose-free maltose in water) just before pouring the plates. Ampicillin (100 μg/ml), kanamycin (50 μg/ml), and IPTG (500 μM) were also added just prior to pouring. All plates were stored at 4°C until used.

Bacterial strain construction

Bacterial strains BW25113 (wild type), BW26337 **(**Δ*pstSCAB-phoU::frt),* and BW26390 (Δ*pstB::frt*) were provided by the Coli Genetic Stock Center at Yale University. BTH101 was provided with the Bacterial Adenylate Cyclase Two-Hybrid System Kit (EuroMedex). All other strains were derivatives of these four parent strains created by plasmid transformations (see Transformations). For a list of all bacterial strains used and created in this research, refer to Table 2.

Plasmid construction

The plasmid pRR48 was used for all strain constructions containing the *pstB* gene, aside from those used for two-hybrid analyses described later in Materials and Methods. The pRR48 plasmid contains a $lacO^{id}$ operon and P_{tac} promoter, regulated by IPTG, and a multiple cloning site for gene ligation. For selection purposes, pRR48 codes for ampicillin resistance (see Fig. 2).

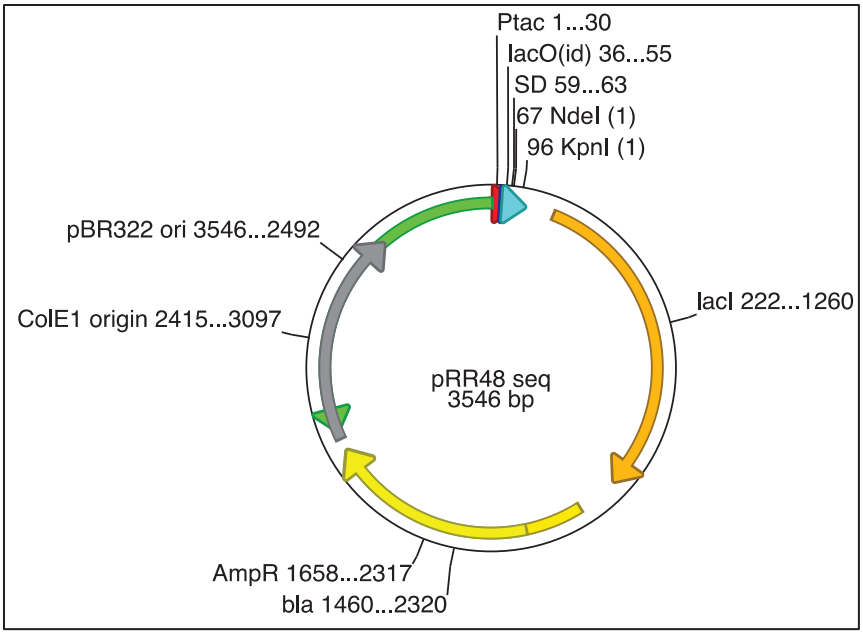

Figure 2. Plasmid map of pRR48.

The pRR48 plasmid is a derivative of pCJ30 (79). This plasmid contains a P_{tac} promoter as well as a lacO id operator upstream a multiple cloning site. Proteins of interest were ligated using the *KpnI* and *NdeI* sites. For selection purposes, the plasmid codes for ampicillin resistance. Gene expression is regulated with IPTG.

For plasmid construction, the *pstB* gene was amplified with PCR, using the wild type *E. coli* strain BW25113 as template. Forward and reverse primers used for amplification are found in Table 1. The restriction sites *NdeI* and *KpnI* were used in the forward and reverse primers, respectively, with the *NdeI* restriction site properly framed to use its ATG sequence to initiate *pstB* expression. For co-purification purposes, a His-tagged version of *pstB* was designed by adding a C-terminal 6X histidine tail to *pstB* using the previous *pstB* forward primer along with a reverse primer containing six histidine coding sequences directly upstream the *pstB* stop codon (see Table 1 for primers; see Fig. 3 for *pstB*-His DNA sequence). Following PCR, amplified DNA was cleaned with a QIAquick PCR Purification Kit and digested using *KpnI* and *NdeI* restriction enzymes.

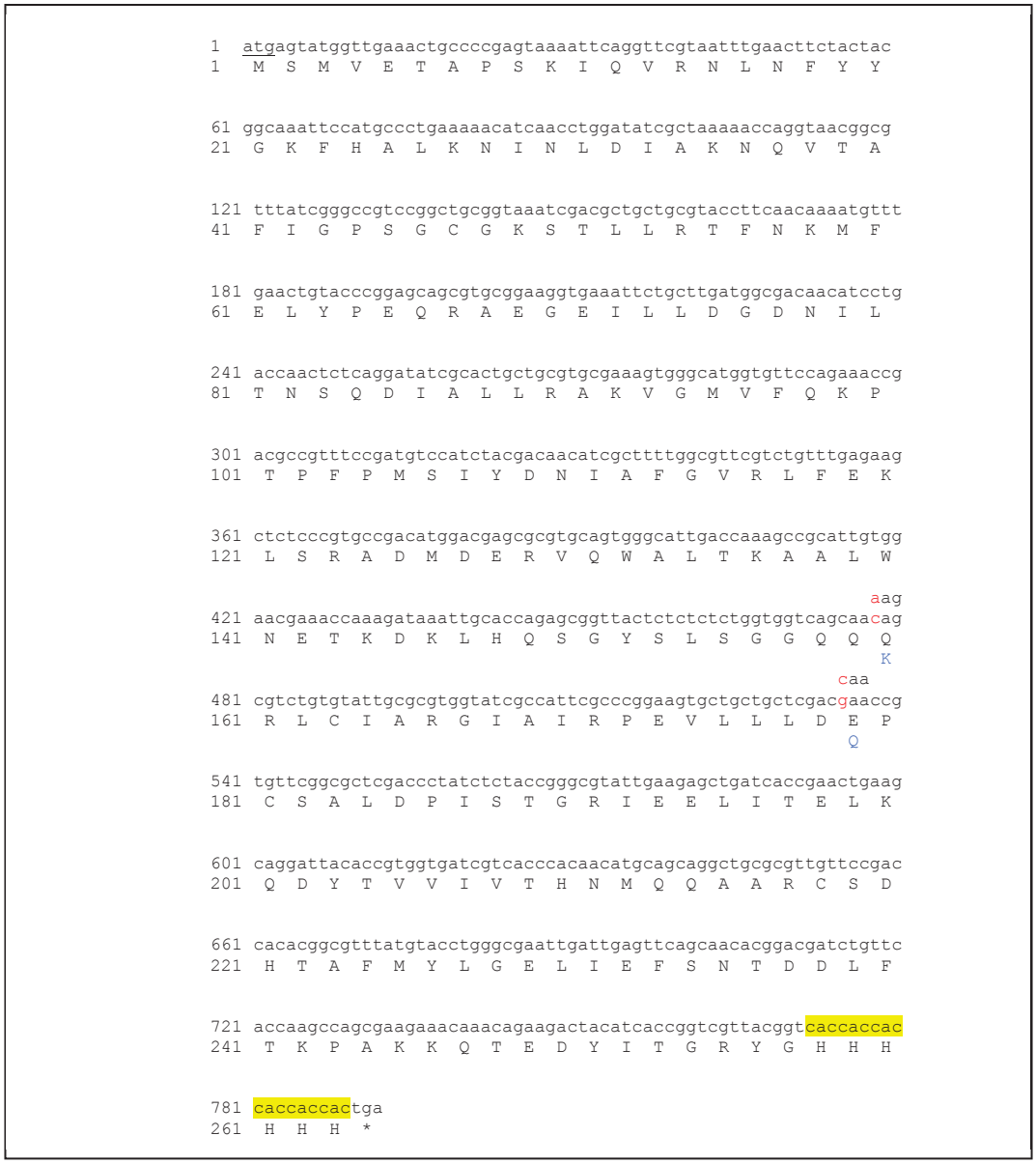

Figure 3. Gene sequence of *pstB*-His

The *pstB*-His nucleotide sequence in *Escherichia coli* with corresponding one letter amino acid translation below each codon. The start codon is underlined; the stop codon is noted with an asterisk in the place of an amino acid. Added histidine sequences are highlighted in yellow. Sites for Q160K and E179Q mutations are lettered in red, with the new codon sequence written above and the amino acid change below in blue lettering.

Restriction digests were done separately for PCR product and plasmid pRR48 DNA using the same protocol. Each sample used the following combinations: 5 µl 10X NEB 1 Buffer, 0.5 µl BSA, 42.5 µl DNA (PCR product or plasmid), 1 µl *NdeI*, and 1 µl *KpnI*. Combined samples were incubated overnight at 37°C. Following incubation, the plasmid digest was treated with 1 µl Antarctic phosphatase and 5.5 µl 10x AP Buffer and left at 37°C for 15 min, after which the Antarctic phosphatase was heat inactivated for 5 min in a 65°C water bath. Plasmid DNA was cleaned using the QIAquick PCR Purification Kit, and both PCR and plasmid DNA were run on an agarose gel to assess digest effectiveness. Once verified, digested PCR and plasmid DNA were ligated by combining 2 µl 10x Buffer, 1 µl T4 DNA Ligase, 5 µl digested plasmid, and 12 µl digested PCR product and allowing the mixture to incubate at room temperature for 10 min. With this process the following plasmids were created: p48-*pstB,* p48-*pstB*-His, p48-*pstB*-E179Q-His, and p48-*pstB*-Q160K-His. For a complete list of plasmids used in this research see Table 2.

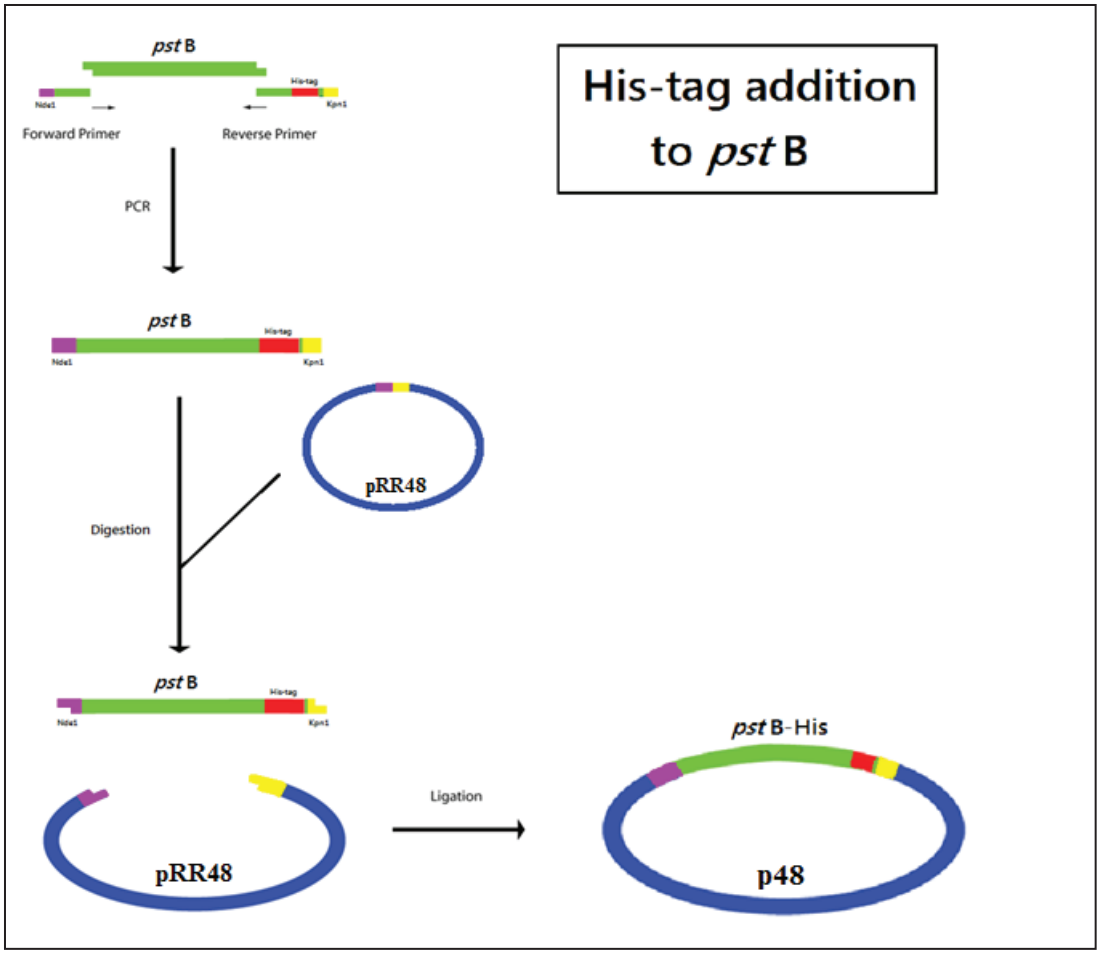

Figure 4. Hig-tag addition overview

Addition of a 6X histidine tag to *pstB* was accomplished using designed forward and reverse primers. The forward primer coded for an *NdeI* restriction site directly upstream the *pstB* complementary start sequence properly framed to provide the ATG start codon. The reverse primer contained complementary *pstB* end sequence followed by six histidine-coding codons, a stop codon, and the *KpnI* restriction site. Chromosomal *pstB* was used as template for PCR amplification. Digested pRR48 plasmid and PCR product were ligated to form a complete vector coding for *pstB*-His.

Mutant construction

Point mutations were made using the QuikChange II Site-Directed Mutagenesis Kit (see Fig. 5 for overview). Plasmid p48-*pstB*-His DNA was amplified through PCR using forward and reverse primers designed to introduce nucleotide changes to the 160th amino acid of PstB, while another set of primers were introduced to produce nucleotide changes in 179th amino acid of PstB (refer to Table 1 for primer design). Both mutations were done separately. The following concentrations were prepared for 50 µl reactions: 10 µl 5X Phusion HF Buffer, 1 µl of 10 mM dNTPs, 2.5 µl of 10 µM forward primer, 2.5 µl of 10 µM reverse primer, and 5-15 µl plasmid DNA (dependent on DNA concentration) with the necessary amount of ddH_20 to total 50 µl. PCR reactions were assembled while on ice and promptly transferred to the PTC-300 Peltier Thermal Cycler for amplification. Program method was run as follows: Step 1. 98.0°C for 30 sec; Step 2. 98.0°C for 10 sec; Step 3. 72.0°C for 20 sec; Step 4. repeat Step 2 – Step 3 for 34 rounds; Step 5. 72.0°C for 5 min; Step 6. 4.0°C forever. After amplification, PCR products were treated with the restriction endonuclease, *DpnI*, in order to cleave the methylated template DNA and leave behind the p48-*pstB*-His plasmid mutants. PCR product was cleaned using the QIAquick PCR Purification Kit prior to digestion.

Mutant plasmids were transformed into NEB 5-alpha competent *E. coli* cells (New England BioLabs). 50 µl of thawed competent cells were mixed with 1-4 µl plasmid DNA and placed on ice for 30 min. The cells were then heat shocked in a 42°C water bath for 30 sec and promptly placed back on ice for 5 min. After 5 min, 950 µl SOC liquid media was added to the cells and the tubes were incubated on a shaker table at 37°C for 1 hr. The samples were plated at various volumes onto LB agar plates containing the appropriate antibiotic and incubated overnight at 37°C. Individual colonies from the plated transformations were streaked onto new plates, with

several colonies from those plates chosen for sequencing to verify mutations. Plasmids purifications from selected colonies were done using a QIAprep Miniprep Kit. Sequencing reactions were made by combining 1 µl of 20 mM primer (one reaction containing a *pstB* forward primer, the other containing a *pstB* reverse primer) with 9 µl plasmid DNA (see Table 1 for primer sequences). Sequencing was processed at the BYU DNA Sequencing Center, and results were compared to wild-type *pstB* sequence to check for proper mutations.

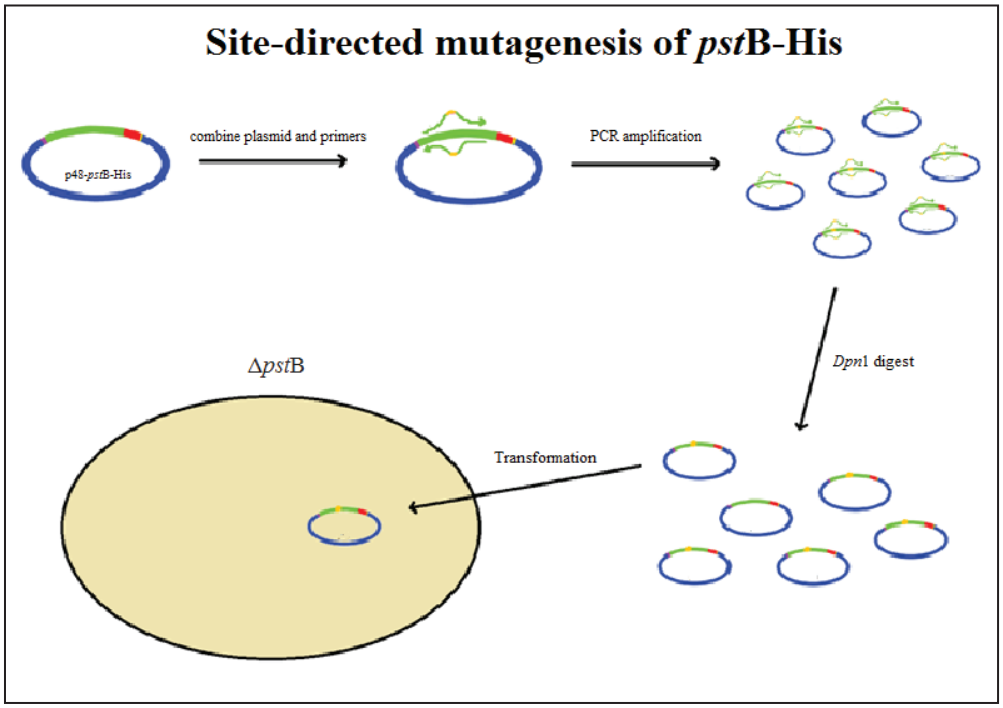

Figure 5. Site-directed mutagenesis overview

The *pstB*-His gene was mutated using plasmid p48-*pstB*-His DNA as template. Separate primers were designed for E179Q and Q160K mutations, and p48-*pstB*-His DNA was amplified using PCR. PCR product was treated with *Dpn*I restriction endonuclease in order to remove the original, non-mutant template DNA. Mutant p48 plasmids were separately transformed into a Δ*pstB E. coli* strain.

DNA electrophoresis

DNA was analyzed on agarose gels comprised of 1X TAE buffer mixed with 0.7% agarose and 2-3 μl ethidium bromide (10 mg/ml), and separated by applying 75 V to the gel for 45-60 min. Gels were imaged in the BYU RIC facility using a BioRad Flour-S Multimager.

Transformations

Competent cells for transformations were prepared from overnight cultures grown in LB growth media containing the appropriate antibiotics. Overnight samples were diluted 1:100 in 25 ml of liquid LB and incubated on a shaker table at 37°C until the culture reached an OD_{600} measurement between 0.3-0.4. Cells were then pelleted in a Sorvall RC 5C Plus centrifuge for 10 min at 9000 rpm at 4°C using the SLA-600TC rotor. After removing the supernatant, the pellet was resuspended in 5 ml of chilled 0.1 M $CaCl_2$ and left on ice for 30 min. After 30 min, cells were pelleted once more (using the same centrifuge settings) and resuspended in 1 ml of 0.1 M $CaCl_2$ (immediate use) or 1 ml of 0.1 M $CaCl_2$ with 15% glycerol (storage in -80°C).

Transformations were carried out by mixing 1 – 4 μl plasmid DNA with 100 – 200 μl thawed competent cells in a sterile, chilled microcentrifuge tube. The tubes were kept on ice for 30 min. An additional "no DNA" sample was included as negative control. After 30 min, the tubes were transferred into a 42°C water bath, heat shocked for 1 min, and then immediately transferred back on ice for 2 min. 1 ml of LB was added to each tube and the samples were allowed to recover for 45-60 min at 37°C. LB plates (with the appropriate antibiotic for selection) were used to culture successfully transformed cells.

Alkaline phosphatase assays

To determine protein functionality, triplicate samples of each strain were cultured overnight at 37°C in 3 ml of LB containing the appropriate antibiotic(s). Once fully cultured, 1 ml of each sample was transferred into a clean microcentrifuge tube and spun down for 2 min using a tabletop centrifuge. The remaining cell cultures were kept on ice until their optical density at 600 nm (OD_{600}) could be measured with a BioRad spectrophotometer (LB blank for LB samples, ddH_2O blank for MOPS samples). After centrifugation, the supernatant was aspirated from each tube, leaving the pelleted cells undisturbed. The pellets were resuspended in 900 µl 1 M Tris-HCl pH 8.2, and 2 drops of chloroform and 1 drop of 0.1% SDS were added to each tube. A blank containing only 900 µl Tris-HCl pH 8.2, 2 drops of chloroform, and 1 drop of 0.1% SDS was also prepared. Each tube was vortexed for 30-60 sec to disrupt the outer membrane.

Alkaline phosphatase reactions were initiated by adding 100 µl of 20 mM para-nitrophenyl phosphate (PNPP) to each tube. The samples were incubated in a 37°C water bath until they reached a solid yellow color, at which point the reactions were stopped by adding 400 µl $KHPO_4$ to the solution. Once the reaction was stopped, the tube was placed on ice. The amount of time between initiation and conclusion of each reaction was recorded during this process. Once all reactions (including the blank) were completed, the samples were centrifuged for 2 min in a tabletop centrifuge (to pellet cell debris and chloroform) and OD_{420} measurements were taken on the top 1 ml of each sample using a BioRad spectrophotometer. Arbitrary AP units (which are analogous to the widely used Miller Units for β-galactosidase activity) were assigned to each sample using the following equation: $\text{AP Units} = (1000*OD_{420})/ (\Delta T(\text{min})*OD_{600})$

Nickel column chromatography

Cultures were grown overnight in 250 ml MOPS LoP$_i$ medium (except the mixed culture which combined the Δ*pstB* strain containing pRR48 in 125 ml MOPS HiP$_i$ with the Δ*pstB* strain containing p48-*pstB*-His in 125 ml MOPS LoP$_i$). All cultures were grown in media containing the proper antibiotic(s). Overnight samples were pelleted using the Sorvall RC 5C Plus centrifuge (15 min at 70000 rpm at 4°C using the GSL rotor) and stored at -20°C. Cell pellets were thawed on ice and resuspended in 5 ml lysis buffer (50 mM Tris-HCl pH 7.2, 300 mM NaCl, 20 mM Imidazole in ddH_2O). Cells were lysed once at 4000 psi, and three additional times at 8000 psi using a Microfluidics cell disruptor. An aliquot of the crude lysate (0.5 ml) was pipetted into a sterile microcentrifuge tube and stored at -20°C for later analysis. The remaining crude lysate was loaded onto a HisTrap FF nickel column (GE Healthcare) using an Econo Pump (BioRad). Flow-through from this process was collected in a 15 ml test tube and stored at -20°C as well. The nickel column was then loaded onto a GE Healthcare AKTA Prime Plus liquid chromatography machine. The following program was used to wash the column and elute PstB with its interacting proteins: a 20 ml wash with 100% lysis buffer (50 mM Tris-HCl pH 7.2, 300 mM NaCl, 20 mM Imidazole in ddH_2O) followed by a 20 ml elution with 100% elution buffer (50 mM Tris-HCl pH 7.2, 300 mM NaCl, 250 mM Imidazole in ddH_2O). Washes and elutions were caught in 1 ml fractions and stored at -20°C. Refer to Fig. 6 for method overview.

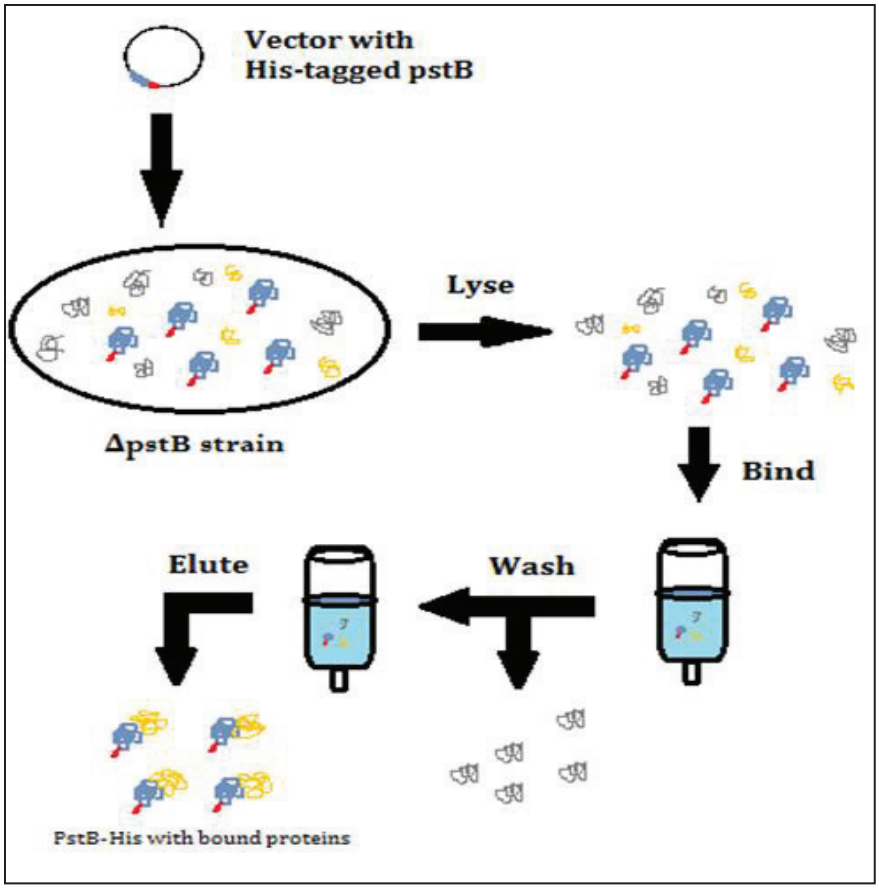

Figure 6. Overview of nickel chromatography co-purification

A p48-*pstB*-His vector was transformed into a Δ*pstB* strain. These cells were lysed and the supernatant fraction was separated on a nickel column. The His-tag on PstB exhibits high affinity for the nickel beads, binding PstB, as well as any interacting proteins, to the column. The column was then washed to remove all unbound protein. Washing the column with a high concentration of imidazole eluted bound protein. Collected fractions were analyzed with Western immunoblotting..

Western blotting

Samples from co-elution runs were analyzed using the Chemiluminescent Western Blot Immunodetection Kit (Invitrogen life technologies). Co-elution fractions were thawed on ice and 50 µl of the sample were mixed with 50 µl Laemmli Sample Buffer in sterile microcentrifuge

tubes (all samples were diluted 1:2 except crude fraction which were diluted 1:50 due to high protein concentration). Diluted samples were boiled for 10 min before being load into the SDS-polyacrylamide gel lanes. The PAGE was run at 200 V for 38 min after which the gel was removed and placed onto a nitrocellulose membrane (BioRad). Protein transfer was run at 100 V for 1 hr. Following transfer, the nitrocellulose membrane was incubated in 10 ml blocking solution for 30 min (same day procedure) or overnight at 4°C (two day procedure). After decanting the blocking solution, the membrane was washed twice with ddH_2O for 5 min and incubated for 1 hr in primary antibody solution (7.5 µl appropriate antibody—α-His for PstB, α-PhoU for PhoU—added to 10 ml blocking solution). Before adding the secondary antibody solution (10ml), the membrane was washed four times with 20 ml of antibody wash solution. Secondary antibody solution was added to the nitrocellulose membrane (mouse antibody for α-His, rabbit antibody for α-PhoU) and allowed to incubate for 30 min. This was followed with four more 5 min 20 ml antibody washes and three final 2 min 20 ml ddH_2O washes. After decanting the last ddH_2O wash, the nitrocellulose was transferred onto a sheet of transparency plastic and 2.5 ml of chemiluminescent substrate was added to the membrane. The substrate was kept on the membrane for 5 min to allow the reaction to develop and then carefully blotted off. The nitrocellulose was covered with another transparency plastic and taken to the dark room for development. X-ray film was exposed to the membrane for varying lengths of time (2-15 min) prior to development, in order to allow adequate band development. The Western blot on crude cell lysate from each strain was run using the same protocol.

Bacterial two-hybrid screen

Two-hybrid screens were carried out using the plasmids pKT25 and pUT18C (see Fig. 7 and Fig. 8) provided by the Bacterial Adenylate Cyclase Two-Hybrid System (BACTH) Kit (EuroMedex). Control plasmids, coding for T18 and T25 fragments containing a leucine zipper (GCN4), were also provided by the BACTH System Kit. Production of plasmid constructs coding for *pstB* and *phoU* were accomplished using the protocol described earlier in Plasmid Construction (using *XbaI* and *KpnI* cloning sites for ligation). PCR amplification for cloning was accomplished using p48-*pstB*-His plasmid DNA and chromosomal *phoU* DNA as template. Plasmid strains coding for mutant *pstB* (E179Q and Q160K) were created through site-directed mutagenesis of the pUT18C-*pstB*-His plasmid. For an overview of the BACTH system, refer to Fig. 9.

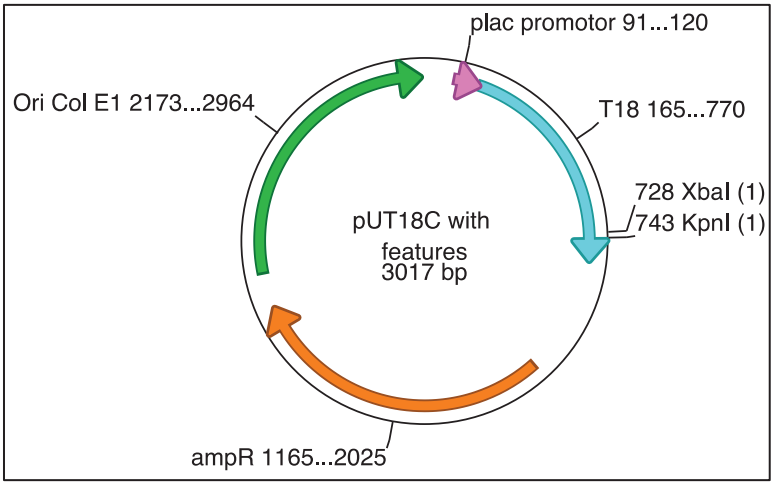

Figure 7. Plasmid map of pUT18C

The pUT18C plasmid is provided by the BACTH System Kit (EuroMedex). Transcription of the T18 fragment of adenylate cyclase is controlled by a lac promoter. The plasmid codes for ampicillin resistance and contains a multiple cloning site located near the 3' end of the T18 open reading frame. Proteins of interest were ligated using the *XbaI* and *KpnI* restriction sites.

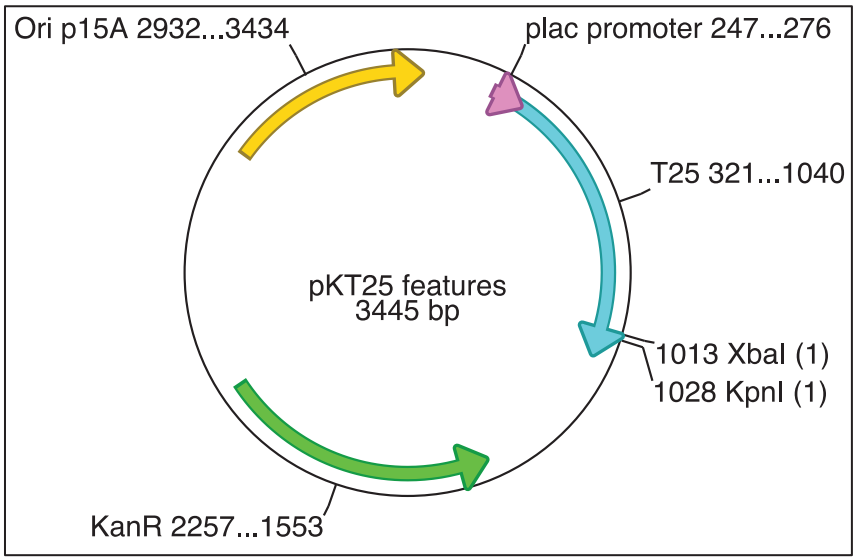

Figure 8. Plasmid map of pKT25

The pKT25 plasmid, provided by the BACTH System Kit, codes for the T25 fragment of adenylate cyclase (EuroMedex). It has a multiple cloning site directly upstream the T25 open reading frame, and is regulated by a lac promoter. Proteins of interest were ligated using the *XbaI* and *KpnI* sites. For selection purposes, the plasmid codes for kanamycin resistance.

Constructed plasmids were co-transformed into BTH101 competent cells and plated onto LB X-gal plates containing 500 μM IPTG and appropriate antibiotics. Transformants were screened onto MacConkey/maltose plates and incubated for 24-72 hr at 30°C. After incubation, screening plates were checked for the presence of red colonies, an indicator of protein-protein interaction. Plates were photographed and stored at 4°C.

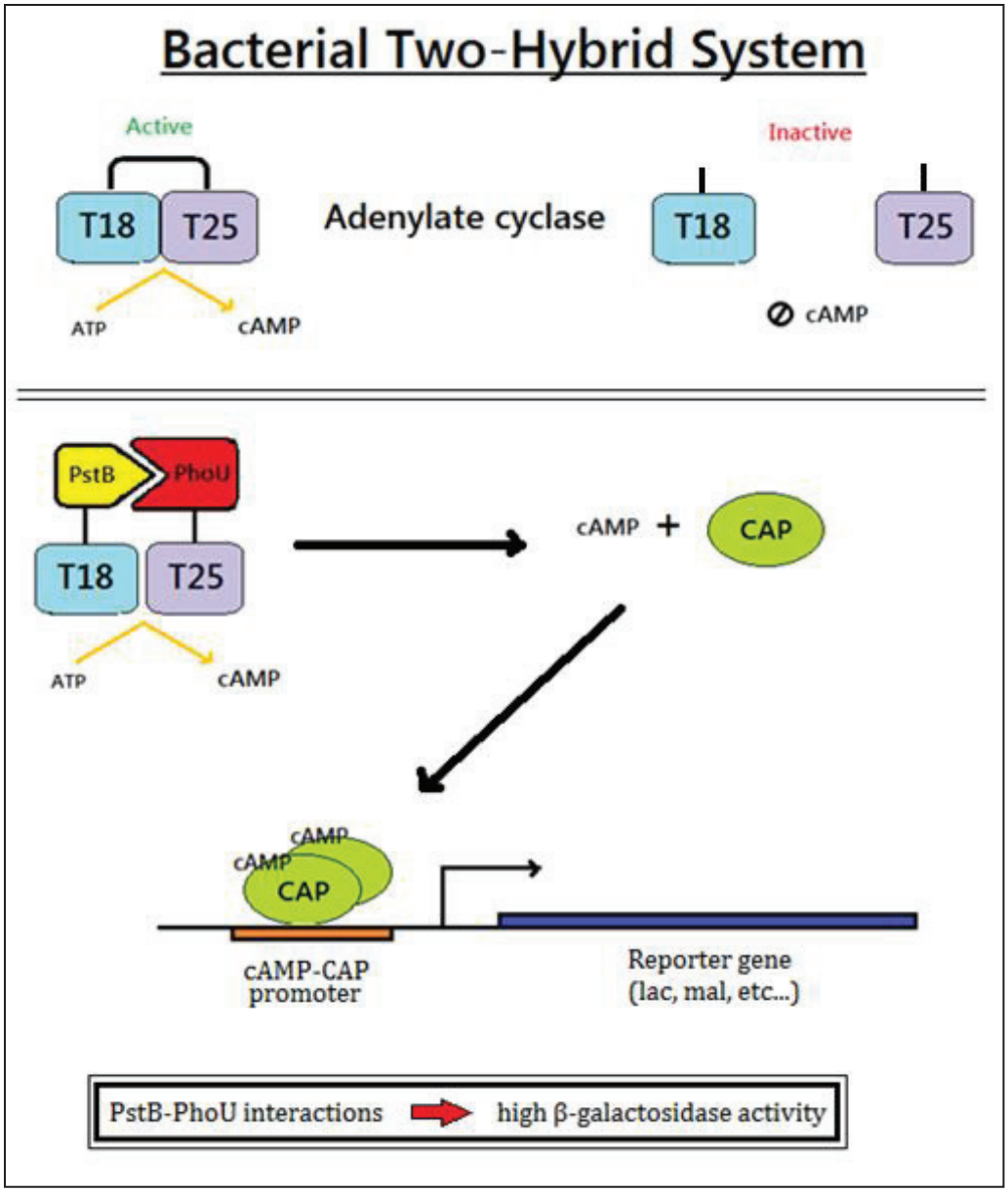

Figure 9. Bacterial adenylate cyclase two-hybrid system overview

The BACTH system uses the two catalytic domains (T18 and T25) of adenylate cyclase to test for protein-protein interactions. When the two domains interact they are able to convert ATP to cAMP. Produced cAMP molecules will bind to CAP transcription factors, which will dimerize and bind to the cAMP-CAP promoter, upregulating expression of reporter genes. Direct protein interactions between PstB and PhoU were verified using this system.

β-galactosidase assays

In order to quantify the efficiencies of hybrid protein interactions, β-galactosidase activity assays were employed. Triplicate samples of each strain were grown overnight at 37°C in 5 ml of LB containing the appropriate antibiotic(s). Overnight samples were chilled on ice for 20 min, diluted 1:10 in sterilize water (0.9 µl ddH_2O with 0.1 µl cells), and the optical density at 600 nm (OD_{600}) was measured using a BioRad spectrophotometer. A ZS-buffer was prepared with the following materials: 16.1 g Na_2HPO_4, 5.5 g NaH_2PO_4, 10.0 ml 1 M KCl, 1.0 ml 1 M $MgSO_4$, 2.7 ml β-mercaptoethanol, and 985 ml ddH_2O. In a fresh microcentrifuge tube, 500µl cell culture was mixed with 500 µl ZS-buffer along with 2 drops of chloroform and 1 drop of 0.1% SDS to permeabilize the cells. The tubes were vortexed for 5 sec and incubated in a 30°C water bath for 2 min. Reactions were started by adding 200µl O-nitrophenol-beta-galactoside (ONPG) at a 4 mg/ml concentration. The reaction continued at 30°C until a sufficient yellow color developed, at which time 500 µl 1M Na_2CO_3 was added to stop the reaction. The amount of time between initiation and conclusion of each reaction was recorded, and a blank containing 1 ml ZS-buffer, 200 µl ONPG, and 500 µl Na_2CO_3 was prepared for optical density readings. After the reactions were completed, all samples were centrifuged for 2 min in a tabletop centrifuge in order to pellet cell debris and chloroform. A 1:5 dilution (1 ml centrifuged reaction with 4 ml ZS-buffer) was prepared for OD_{420} and OD_{550} readings using the prepared blank as control. Miller units were calculated for each sample using the following equation: Miller Units = $(1000*(OD_{420}-(1.75*OD_{550}))/ (\Delta T(min)*v*OD_{600})$.

Phosphate transport assay

In order to measure uptake levels of radioactively labeled inorganic phosphate ($^{32}P_i$), duplicate samples of each strain were cultured overnight in 5 ml of MOPS low phosphate medium. Overnight samples were pelleted and resuspended in an equal volume (5 ml) of MOPS no phosphate medium. Cells were incubated for 2 hr at 37°C to induce phosphate starvation and then diluted into MOPS no phosphate media to an OD_{600} measurement of 0.05 was reached. Following phosphate starvation and dilution, 480 µl of diluted cells were mixed with 20 µl $^{32}P_i$ (25 µM concentration; 2 µCi). Aliquots (200µl) of the mixed samples were pulled at 20 sec and 40 sec time markers and filtered on 0.55 µM nitrocellulose filter discs using the Millipore 1225 Sampling Manifold system. Filtering was accomplished by pipetting the 200 µl aliquot onto the nitrocellulose filter along with a 10 ml TBS (Tris-buffered saline) wash, followed by vacuum-induced filtration. Filtered cells were measured for radioactivity by scintillation counting (see Figure 10 overview).

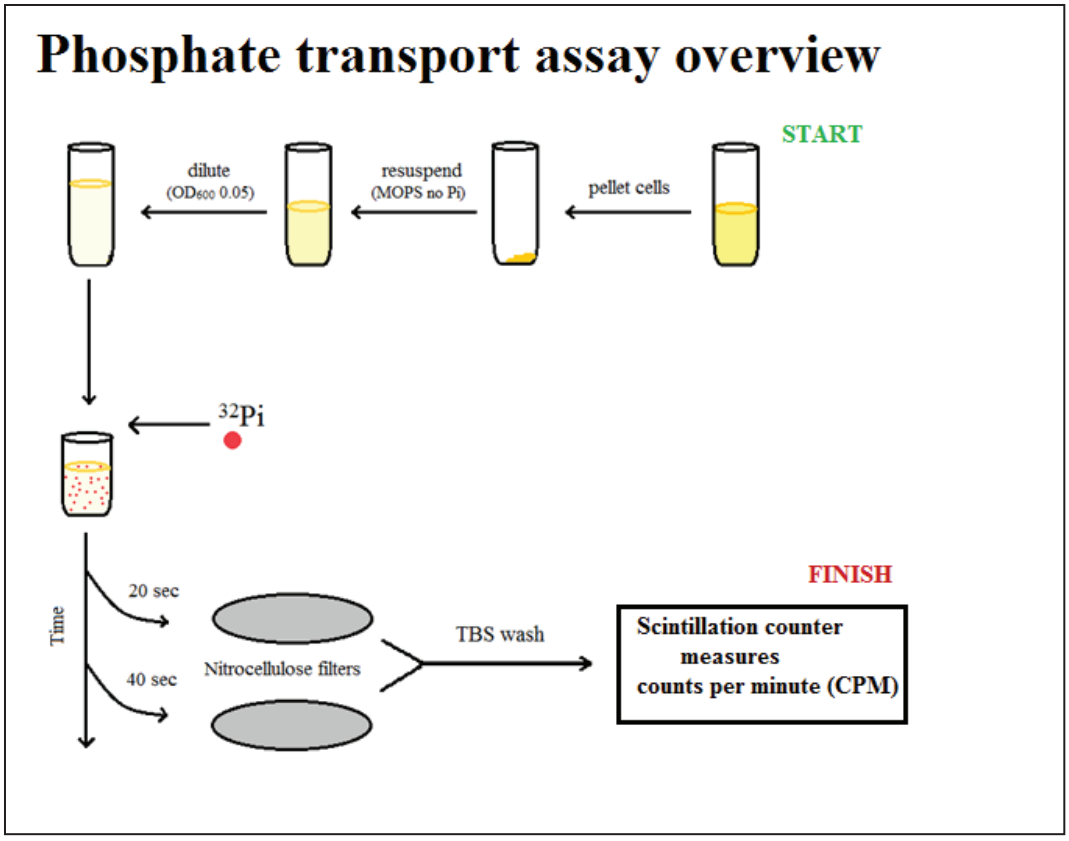

Figure 10. Phosphate transport assay overview

Strains were cultured overnight in MOPS low phosphate medium, pelleted and resuspended in MOPS no phosphate medium to induced phosphate starvation. Following 2 hr incubation in the no phosphate medium, cells were diluted to an OD_{600} of 0.05 and mixed with radioactively labeled phosphate. Aliquots were pulled from each sample at 20 sec time increments and filtered. Filtered cells were measured by scintillation counting.

Table 1. List of PCR primers used in this study

Start codon sequences are underlined. The engineered restrictions sites (*NdeI*, *KpnI*, and *XbaI*) are bolded. His-tag sequences are in lower-case lettering. Nucleotide changes in the mutagenesis primers are labeled in red lettering with the amino acid codon sequence underlined.

Primer name	Sequence in 5'-3' direction
pstB forward (*NdeI*)	GACGCAGGCC**CATATG**AGTATGGTTGAAACTGCCCCGAGTAAAATTCAGG
pstB reverse (*KpnI*)	GACGCAGGCC**GGTACC**TCAACCGTAACGACCGGTGATGTAG
pstB reverse –His (*KpnI*)	GTA**GGTACC**TCAgtggtggtggtggtggtgACCGTAACGACCG
pstB -Q160K forward	TCTCTCTCTGGTGGTCAGCAA**A**AGCGTCTGTGT
pstB -Q160K reverse	ACACAGACGCT**T**TTGCTGACCACCAGAGAGAGA
pstB -E179Q forward	GCTGCTGCTCGAC**C**AACCGTGTTCGGC
pstB -E179Q reverse	GCCGAACACGGTT**G**GTCGAGCAGCAGC
pstB forward (*XbaI*)	GACTGACTGA**TCTAGA**CGGTGGTATGAGTATGGTTGAAACTGCCCCG
pstB -C-term reverse (*KpnI*)	GACTGACTGA**GGTACC**TCAACCGTAACGACCGGTGATGTA
phoU forward (*XbaI*)	GACTGACTGA**TCTAGA**CGGTGGTATGGACAGTCTCAATCTTAATAAACATATTTCCG
phoU reverse (*KpnI*)	GACTGACTGA**GGTACC**TTATTTGTCGCTATCTTTCCCCGCC
pstB -Q160K forward (*XbaI*)	GACTGACTGA**TCTAGA**CGGTGGTATGAGTATGGTTGAAACTGCCCCG
pstB -Q160K reverse (*KpnI*)	GACTGACTGA**GGTACC**TCAACCGTAACGACCGGTGATGTA
pstB -E179Q forward (*XbaI*)	GACTGACTGA**TCTAGA**CGGTGGTATGAGTATGGTTGAAACTGCCCCG
pstB -E179Q reverse (*KpnI*)	GACTGACTGA**GGTACC**TCAACCGTAACGACCGGTGATGTA

Table 2. *E. coli* strains and plasmids used in this study

Strain or plasmid	Description or relevant characteristic(s)	Source or reference(s)
E. coli strains		
BW25113	wild type *E. coli*	CGSC Yale University
BW26337	BW25113 Δ*pstSCAB-phoU::frt*	CGSC Yale University
BW26390	BW25113 Δ*pstB::frt*	CGSC Yale University
BTH101	adenylate cyclase deficient (*cya*) *E. coli* strain	EuroMedex
Plasmids		
pRR48	Am^r, IPTG-induced P_{tac} promoter, lacO	(77)
p48-*pstB*	pRR48 with *pstB*	This study
p48-*pstB*-His	pRR48 with *pstB*-6XHis-tag	This study
p48-*pstB*-Q160K-His	pRR48 with *pstB*-Q160K-6XHis-tag	This study
p48-*pstB*-E179Q-His	pRR48 with *pstB*-E179Q-6XHis-tag	This study
pUT18C	Am^r; IPTG-induced P_{lac} promotor; codes C-term addition of T18	EuroMedex
T18-*pstB*	pUT18C with *pstB*	This study
T18-*pstB*-Q160K	pUT18C with *pstB*-Q160K	This study
T18-*pstB*-E179Q	pUT18C with *pstB*-E179Q	This study
T18-zip	pUT18C with fused leucine zipper to T18	This study
T18-*phoU*	pUT18C with *phoU*	This study
pKT25	Km^r; IPTG-induced P_{lac} promoter; codes C-term addition of T25	EuroMedex
T25-*pstB*	pKT25 with *pstB*	This study
T25-*phoU*	pKT25 with *phoU*	This study
T25-zip	pKT25 with fused leucine zipper to T25	This study

RESULTS

The purpose of our research had three specific aims: first, we hoped to identify direct protein-protein interactions between PstB and PhoU; after which we wanted to determine if the conformational changes of $PstSCAB_2$ affected PstB-PhoU interaction; our final aim was to establish if signal transduction was induced by the transport of P_i into the cell or by conformational changes of $PstSCAB_2$. Both biochemical and genetic approaches were employed to address these aims. Biochemical analyses were carried out by purifying a 6X His-tagged version of PstB using nickel chromatography and assaying for PhoU co-elution by Western blotting with rabbit polyclonal α-PhoU serum. Genetic analyses were accomplished using a bacterial adenlyate cyclase two-hybrid system screening for phenotypic observations of PstB-PhoU protein interactions, which were verified quantitatively using β-galactosidase assays.

Aim 1: Identify direct protein-protein interactions between PstB and PhoU

For co-purification purposes, a C-terminal 6X His-tag was introduced to wild type *pstB* prior to ligation into pRR48. A control vector containing un-tagged *pstB* was also created. Both vectors were separately transformed into a Δ*pstB* strain (BW26390), forming two reconstituted strains, one producing un-tagged wild type *pstB*, the other wild type *pstB*-His. Reconstituted strains were then tested for protein functionality.

Determine functionality of reconstituted PstB and PstB-His

Signaling efficiency of PstB and PstB-His was tested using alkaline phosphatase assays. In high phosphate conditions, both *pstB* and *pstB*-His strains exhibited very low levels of alkaline phosphatase activity, similar to the wild type control, indicating a highly functional signal for both test strains (see Fig. 11). However, in low phosphate conditions, while the

reconstituted *pstB* strain demonstrated an expected increase of alkaline phosphatase activity, the reconstituted *pstB*-His strain exhibited negligible alkaline phosphatase activity (see Fig. 12). These results indicate that the strain reconstituted with native PstB demonstrate functional signaling like the wild type strain, but for reasons unknown, PstB with a C-terminal His-tag causes the cell to constitutively signal regardless of environmental phosphate conditions.

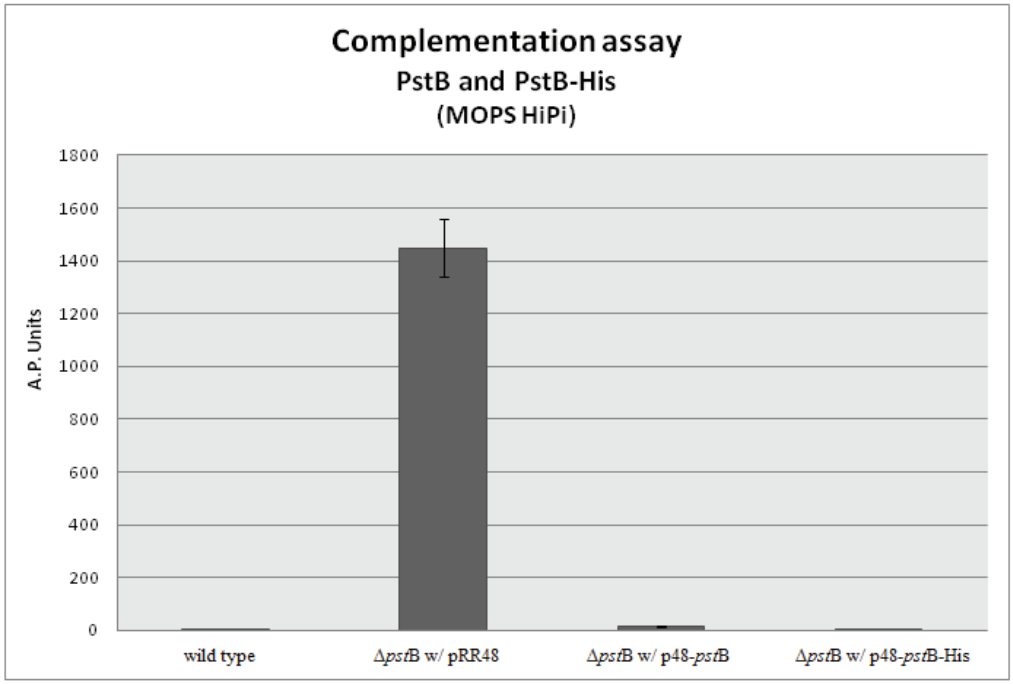

Figure 11: Complementation assay for PstB and PstB-His (MOPS HiP_i)

Alkaline Phosphatase assays were performed on the following strains grown in 1 X MOPS high phosphate medium: wild type, a Δ*pstB* strain with pRR48, a Δ*pstB* strain with p48-*pstB,* and a Δ*pstB* strain with p48-*pstB*-His. Error bars measure the standard deviation for triplicate samples.

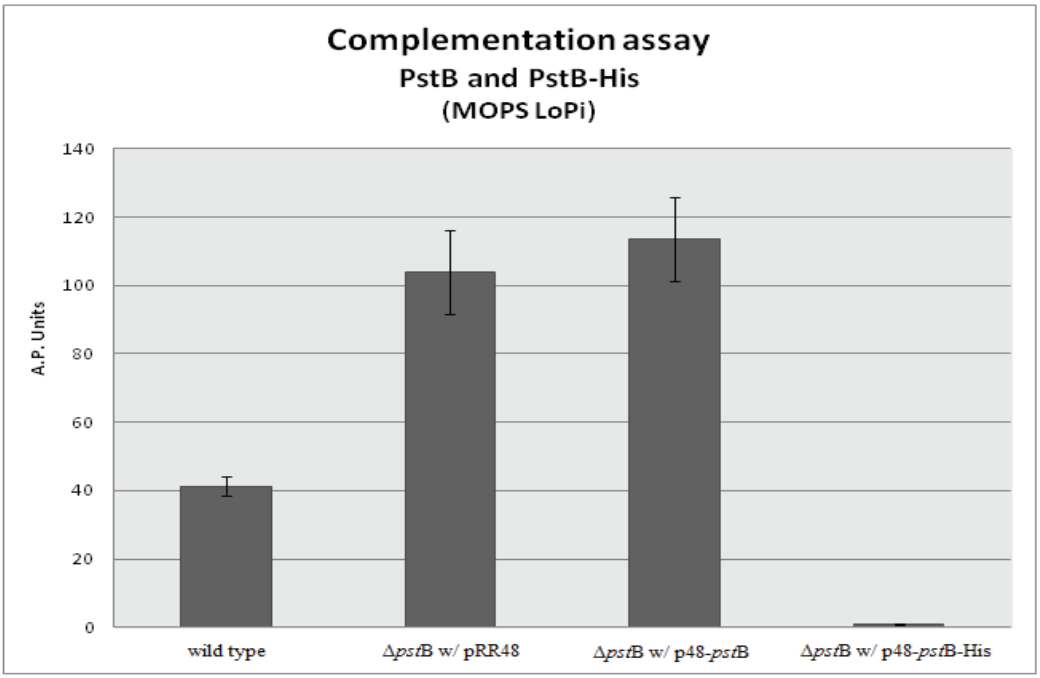

Figure 12: Complementation assay for PstB and PstB-His (MOPS LoP_i)

Alkaline phosphatase assays were performed on the following strains grown in 1 X MOPS low phosphate medium: wild type, a Δ*pstB* strain with pRR48, a Δ*pstB* strain with p48-*pstB,* and a Δ*pstB* strain with p48-*pstB*-His. Error bars measure the standard deviations for triplicate samples.

Establish dominance of chromosomal *pstB* and plasmid-based *pstB*-His expression

To determine to what degree chromosomal *pstB* or the plasmid-encoded *pstB*-His function, a dominance test was conducted comparing the two proteins via alkaline phosphatase assays. For these assays, a test strain was created by transforming the p48-*pstB*-His plasmid into a wild type *E. coli* strain (BW25113). This provided the newly-transformed strain with the capability of expressing chromosomal *pstB* as well as plasmid-encoded *pstB*-His. The unique ability of PstB-His to constitutively signal, even in low phosphate conditions, provided an opportunity to perform a simple comparison to determine dominance. If the wild type strain, which typically produced high alkaline phosphatase activity levels in low phosphate conditions,

began to exhibit low activity levels with an addition of the p48-*pstB*-His plasmid, it would indicate that plasmid-encoded *pstB*-His was dominant to chromosomal *pstB*. However, if signaling was unaffected by the addition of the p48-*pstB*-His vector, then wild-type PstB would be dominant to PstB-His.

As seen in Fig. 13, in low phosphate conditions the wild type strain containing p48-*pstB*-His showed little to no decrease in alkaline phosphatase activity levels compared to the wild type control. These results demonstrate that chromosomal PstB is highly dominant to PstB-His expressed from a plasmid.

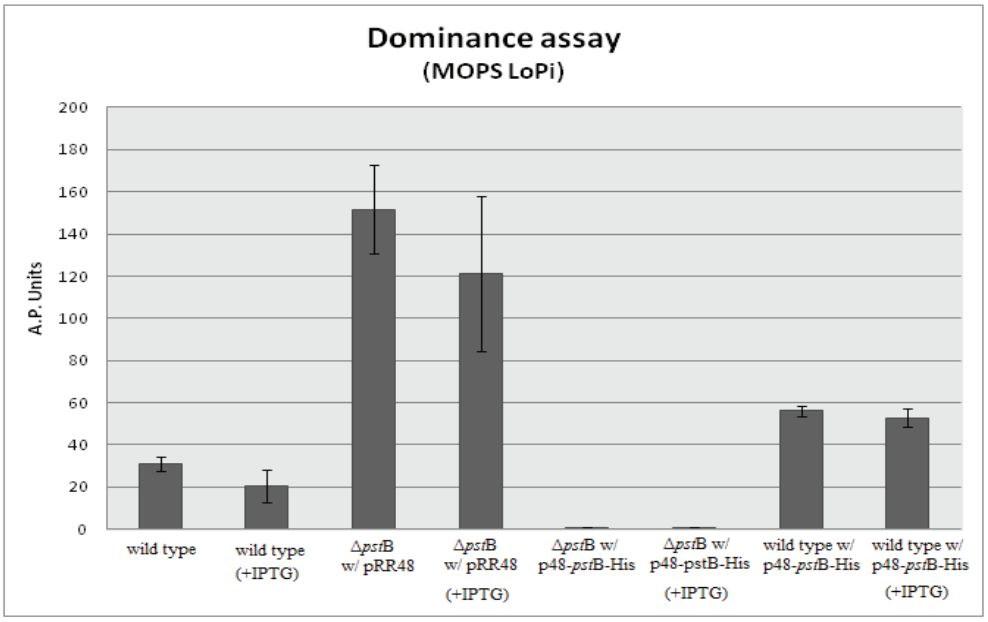

Figure 13. Dominance assay comparing PstB and PstB-His

Alkaline phosphatase assays were performed on the following strains grown in 1 X MOPS low phosphate medium with or without 500 µM IPTG: wild type, a Δ*pstB* strain with pRR48, a Δ*pstB* strain with p48-*pstB*-His, and a wild type strain with p48-*pstB*-His. Error bars measure standard deviations for triplicate samples.

PstB-PhoU interactions observed via co-purification and immunoblotting

Once protein functionality of p48-*pstB* and p48-*pstB*-His was determined, experiments designed to identify potential protein-protein interactions between PstB and PhoU were conducted in order to accomplish our first aim. Protein-protein interactions were first tested using affinity co-purification—purifying His-tagged PstB on a Hi-Trap nickel sepharose column along with any interacting proteins—and then performing an immunoblot on the subsequent crude, wash, and elution fractions searching for the presence of PhoU with eluted PstB-His. Results from our co-purification experiments were then verified using a bacterial adenylate cyclase two-hybrid system.

To determine relative expression levels of PstB and PhoU in the strains used for co-elution experiments, a preliminary Western blot was performed on whole-cell extracts from cells grown in either high or low phosphate conditions (Fig. 14). The Western blot indicated that the Δ*pstB* strain containing p48-*pstB*-His produced very low levels of PstB and PhoU (in low phosphate medium), and exhibited high levels of PstB, but not PhoU (in high phosphate medium) (refer back to Fig. 14). The immunoblot also indicated that the Δ*pstB* strain containing pRR48 produced high levels of PhoU in both high and low phosphate conditions. Given this information a mixed test sample containing the Δ*pstB* strain with p48-*pstB*-His (cultured in MOPS high phosphate medium) and the Δ*pstB* with pRR48 (cultured in MOPS low phosphate medium), was created to ensure adequate expression of both PstB and PhoU. The co-purified mixed sample was analyzed with Western blotting along with two control strains (the Δ*pstB* strain containing pRR48 and the Δ*pstSCAB-phoU* strain containing p48-*pstB*-His).

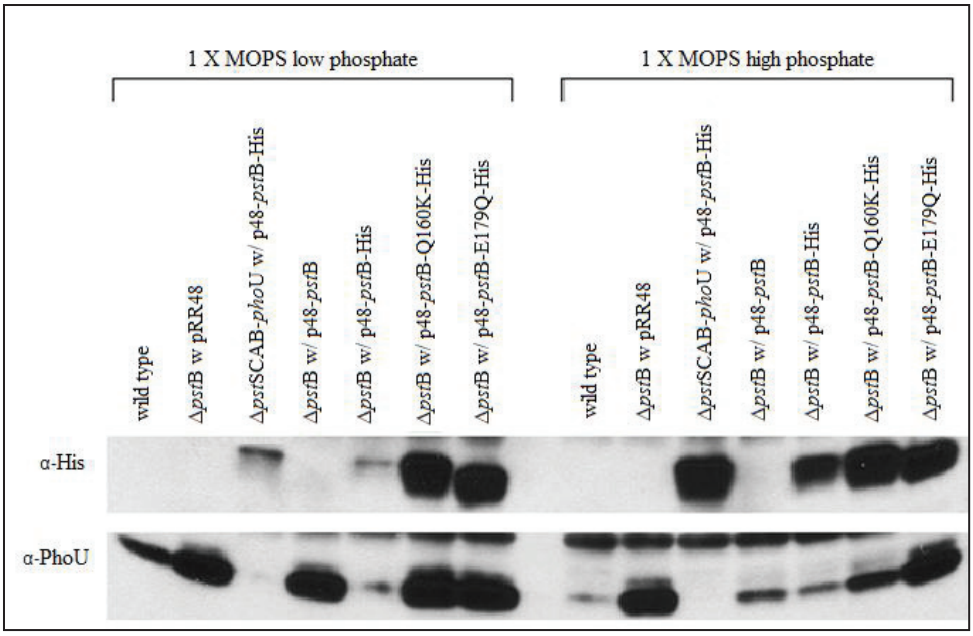

Figure 14. Western blot on whole-cell lysate

The following strains were grown in low or high phosphate media: wild type, a Δ*pstB* strain with pRR48, a Δ*pstSCAB-phoU* strain with p48-*pstB*-His, a Δ*pstB* strain with p48-*pstB*, a Δ*pstB* strain with p48-*pstB*-His, a Δ*pstB* strain with p48-*pstB*-Q160K-His, and a Δ*pstB* strain with p48-*pstB*-E179Q-His. Whole-cell lysates prepared from each strain were separated using SDS-PAGE. Protein for immunoblotting was separately probed with α-His and α-PhoU antibodies.

As seen in Fig. 15, the control Δ*pstSCAB-phoU* strain containing p48-*pstB*-His showed an absence of PhoU in every fraction with weak PstB bands in the crude and elution fractions. These results are consistent with those seen from the whole-cell lysate Western blot, where the Δ*pstSCAB-phoU* strain containing p48-*pstB*-His produced low levels of PstB in MOPS low phosphate (see Fig. 14). The other control Δ*pstB* strain with pRR48 showed an absence of PstB in every fraction and a strong PhoU band found only in the crude, demonstrating that PhoU will not bind to the nickel column in the absence of PstB (Fig.15). The mixed sample showed bands for PstB-His and PhoU in the crude, flow through, and elution fractions, but not in the washes (Fig.15). These results demonstrate that, not only were PstB and PhoU both present in the

sample, but they co-eluted in the same fractions, providing strong evidence for a PstB-PhoU protein-protein interaction.

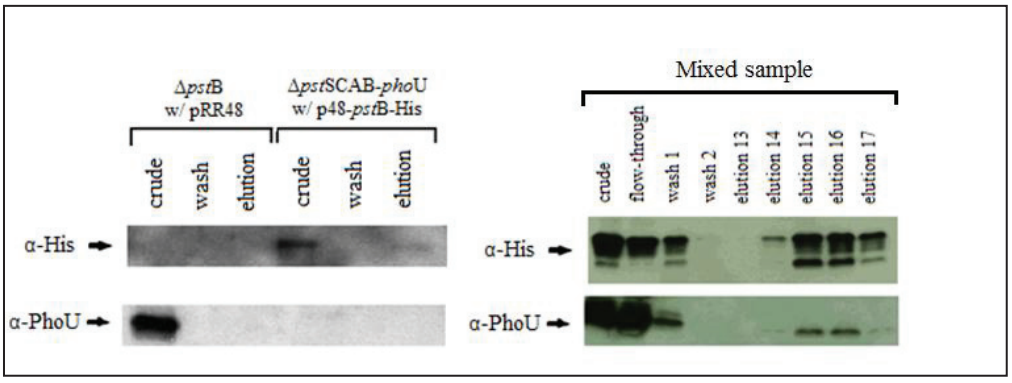

Figure 15. Western blot testing PstB and PhoU interactions

Control strains (a Δ*pstB* with pRR48 and a Δ*pstSCAB-phoU* strain with p48-*pstB*-His) were cultured in low phosphate medium. The mixed strain combined overnight cultures of a Δ*pstB* strain with p48-*pstB*-His (grown in high P_i) and a Δ*pstB* strain with pRR48 (grown in low P_i). Lysed cells were co-purified and protein from selected fractions was separated with SDS-PAGE. Protein was separately probed with α-His and α-PhoU antibodies.

PstB-PhoU interactions verified through two-hybrid system

To verify interactions observed in the co-purification experiments, PstB and PhoU interactions were tested using a bacterial adenylate cyclase two-hybrid (BACTH) system. The BACTH system utilizes adenylate cyclase, an enzyme containing a catalytic domain comprised of two fragments (T18 and T25), which when together are active, but when separated are inactive. By fusing two proteins of interest to these enzyme fragments, protein-protein interactions can be determined by indirectly observing adenlyate cyclase activity in the cell. Adenylate cyclase activity can be observed phenotypically on MacConkey/maltose screening plates; active colonies turn red, inactive colonies remain white. Enzyme activity can also be measured quantitatively using β -galactosidase assays. While this system is not ideal for testing

interactions of complexed proteins in their native state, it is useful in verifying protein-protein interactions between two specific proteins, such as PstB and PhoU.

Co-transformed strains from our experiments were analyzed qualitatively on MacConkey/maltose reporter plates. Phenotypes from these incubated plates exhibited red colonies for the strain containing pUT18C-*phoU* and pKT25-*pstB* as well as the pUT18C-zip and pKT25-zip positive control (see Fig. 16), while colonies from the remaining negative controls remained white. These results provide additional evidence to confirm that protein-protein interactions take place between PstB and PhoU.

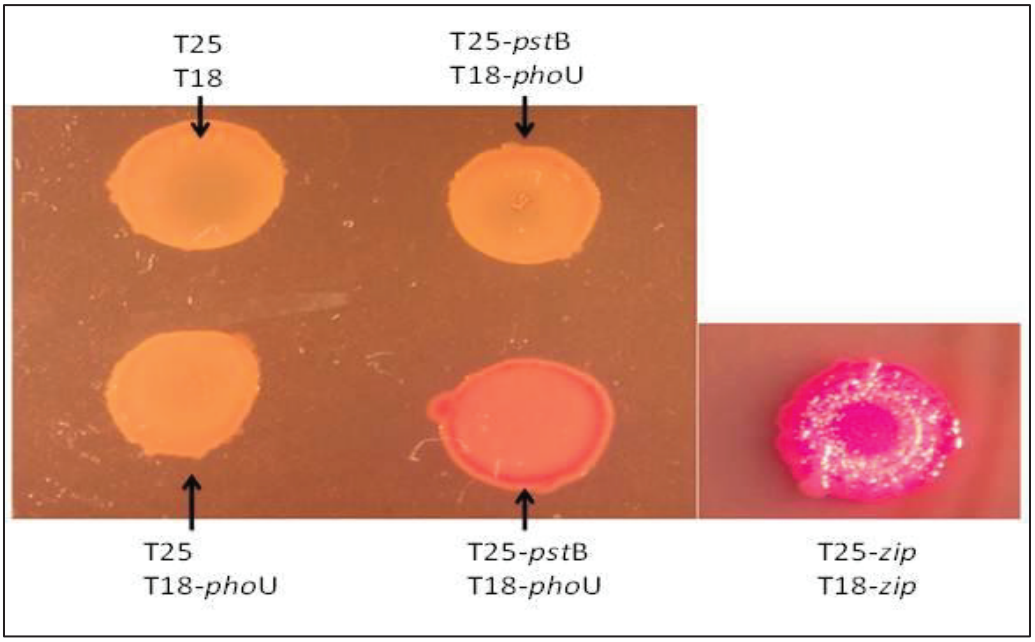

Figure 16. Two-hybrid analysis of PstB-PhoU interactions

Test and control strains were spotted onto MacConkey/maltose plates and incubated at 30°C for 36-48 hr. White colonies indicate no protein interactions; deep red colonies indicate protein-protein interactions.

Results from the two-hybrid screen were quantitatively analyzed with β-galactosidase assays. Results from the assays demonstrated that the strain containing pUT18C-*phoU* and pKT25-*pstB* as well as the swapped-vector strain containing pUT18C-*pstB* and pKT25-*phoU* exhibit β-galactosidase activity levels higher than the negative controls (see Fig. 17). However, the Miller units for these strains were significantly lower than the zip control. These findings may indicate that the interaction between PstB and PhoU is weak. These results could also reflect the fact that PstB normally exists as a dimer of a multi-component transporter and may not adopt a completely native conformation or interaction in these fusion constructs.

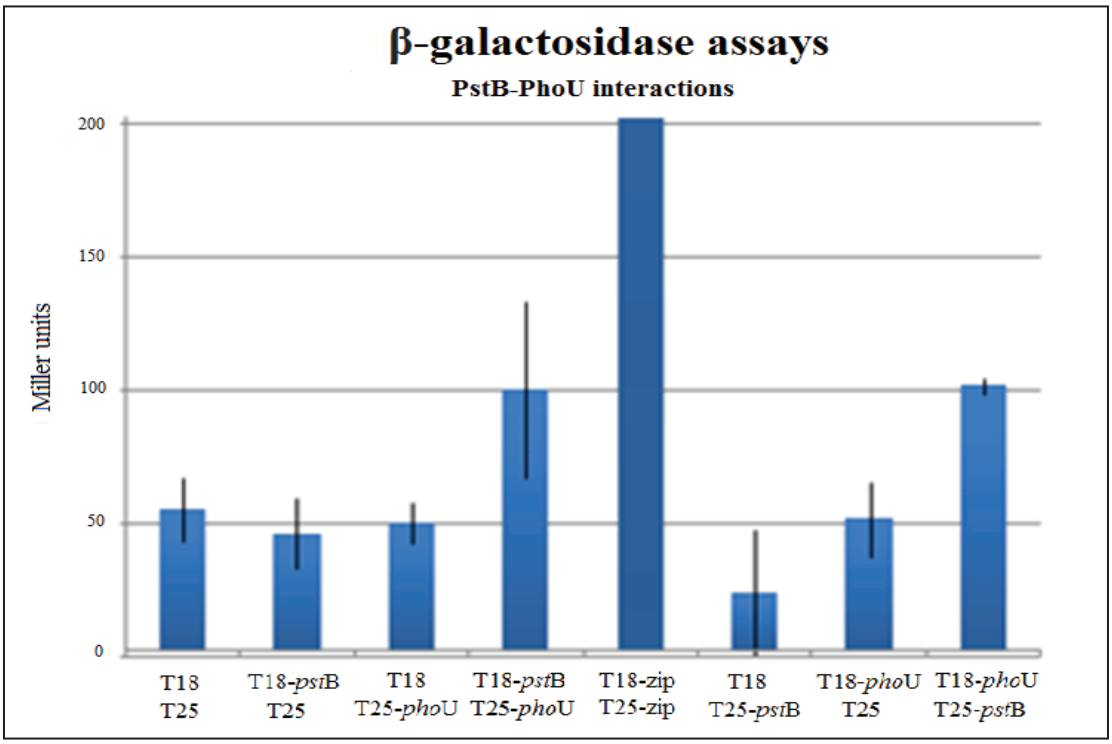

Figure 17. β-galactosidase assays testing PstB-PhoU interactions

β-galactosidase assays were used to quantitatively analyze protein interactions between PstB and PhoU. The following strains were used as negative controls: T25 and T18, T25-*pstB* and T18, and T25 and T18-*phoU*, T18-*pstB* and T25, and T18 and T25-*phoU*. A strain containing T18-zip and T25-zip was used as a positive control. The test strain, T18*pstB* and T25*phoU*, and the swapped-vector test strain, T18*phoU* and T25*pstB*, were compared to positive and negative controls.

Aim 2: Characterize PstB-PhoU interactions with $PstSCAB_2$ conformations

In order to clarify the protein-protein interactions between PstB and PhoU, the next aim was to explore how PstB-PhoU interactions were affected when the $PstSCAB_2$ transporter was 'locked' in open or closed conformations (see Fig.18 for conformation models). In order to lock the transporter in these conformations, point mutations were made to *pstB* which resulted in the alteration of key amino acid residues required for the $PstSCAB_2$ to transition between conformations. Specific mutations for *pstB* were chosen based on previous research for the homolog ABC transporter, $MalFGK_2$. Studies performed by Daus *et al.* determined that mutations in the highly conserved Walker B motif (responsible for ATP hydrolysis) and ABC Signature motif (responsible for stabilizing bound ATP in the sister dimer) of MalK locked the transporter in closed or open states, respectively (for structural location of motifs see Fig. 19) (59). The Walker B mutation switched a negatively charged glutamate to an uncharged glutamine (E158Q), whereas the ABC signature mutation traded an uncharged glutamine for a positively charged lysine residue (Q140K).

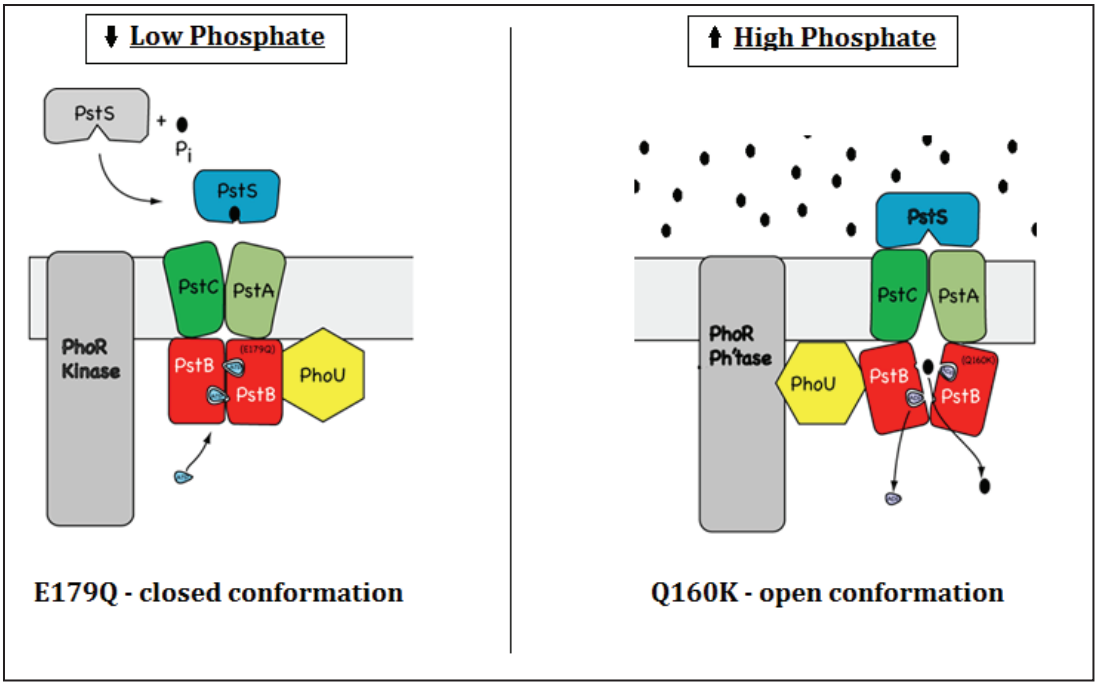

Figure 18. Model of PstSCAB$_2$ signaling conformations

The E179Q mutation in the Walker B motif of PstB is proposed to lock PstSCAB$_2$ in a closed conformation. This mutation prevents the phosphate signal from being transduced to PhoR. The Q160K mutation in the ABC signature motif is believed to lock PstSCAB$_2$ in an open conformation. This mutant complex demonstrates phosphate signaling capabilities. The alternative conformations of PstSCAB$_2$ affect protein-protein interactions between PstB, PhoU, and PhoR.

To identify where similar mutations should be made in PstB, a BLAST alignment comparing PstB with MalK was performed which identified the conserved amino acid motifs in PstB that aligned with the Walker B and ABC Signature motifs of MalK (see Fig. 20). Using site-directed mutagenesis, similar mutations were introduced into the WalkerB and ABC Signature motifs of PstB, namely an E179Q mutation to potentially lock the transporter in a closed conformation and a Q160K mutation to lock it in an open conformation. For co-elution purposes, a 6X His-tag was added to both mutant versions of PstB using the p48-*pstB*-His plasmid as template. Analyses of the two reconstituted mutant strains were carried out using the

same biochemical and genetic approaches as previously performed on the Δ*pstB* strain containing wild type p48-*pstB*-His.

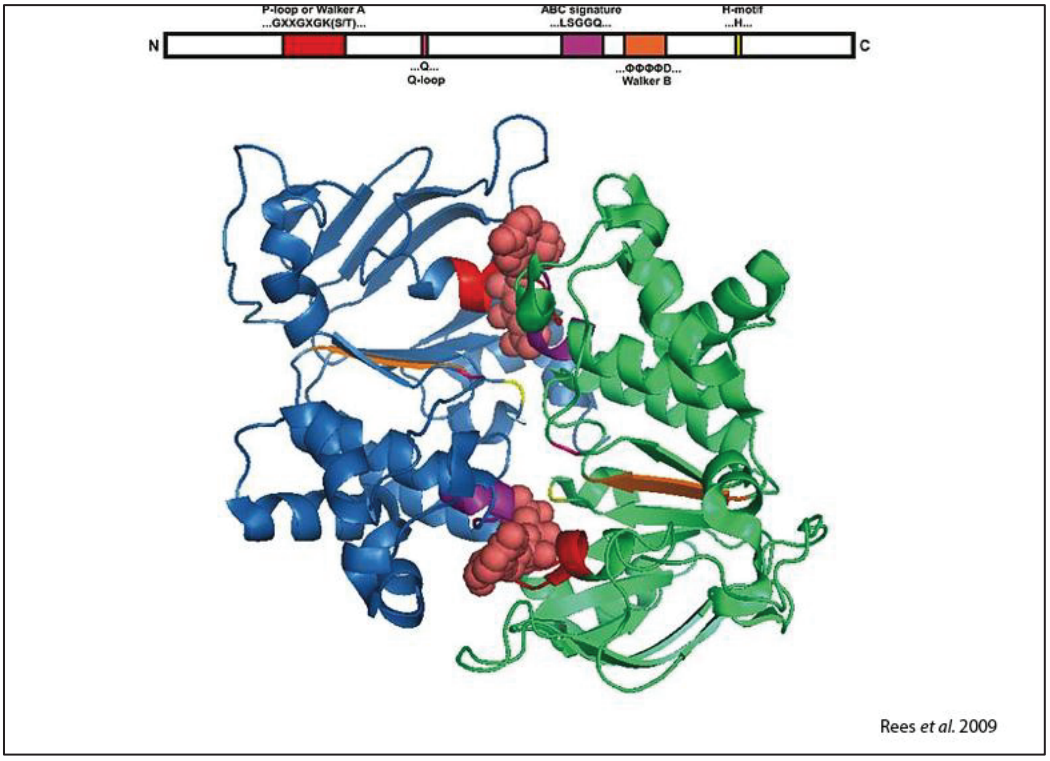

Figure 19: Crystal structure of a PstB dimer homolog (1)

Key motifs are highlighted in the linear sequence located at the top of the page; corresponding motifs are highlighted in the crystal structure below. The Walker A motif, required for ATP binding, is highlighted in red. The Walker B motif, responsible for hydrolyzing ATP, is highlighted in orange. The ABC signature motif, needed to stabilize ATP bound in the sister dimer, is highlighted in purple. The interaction of these key motifs allows the dimer to perform its ATPase activity.

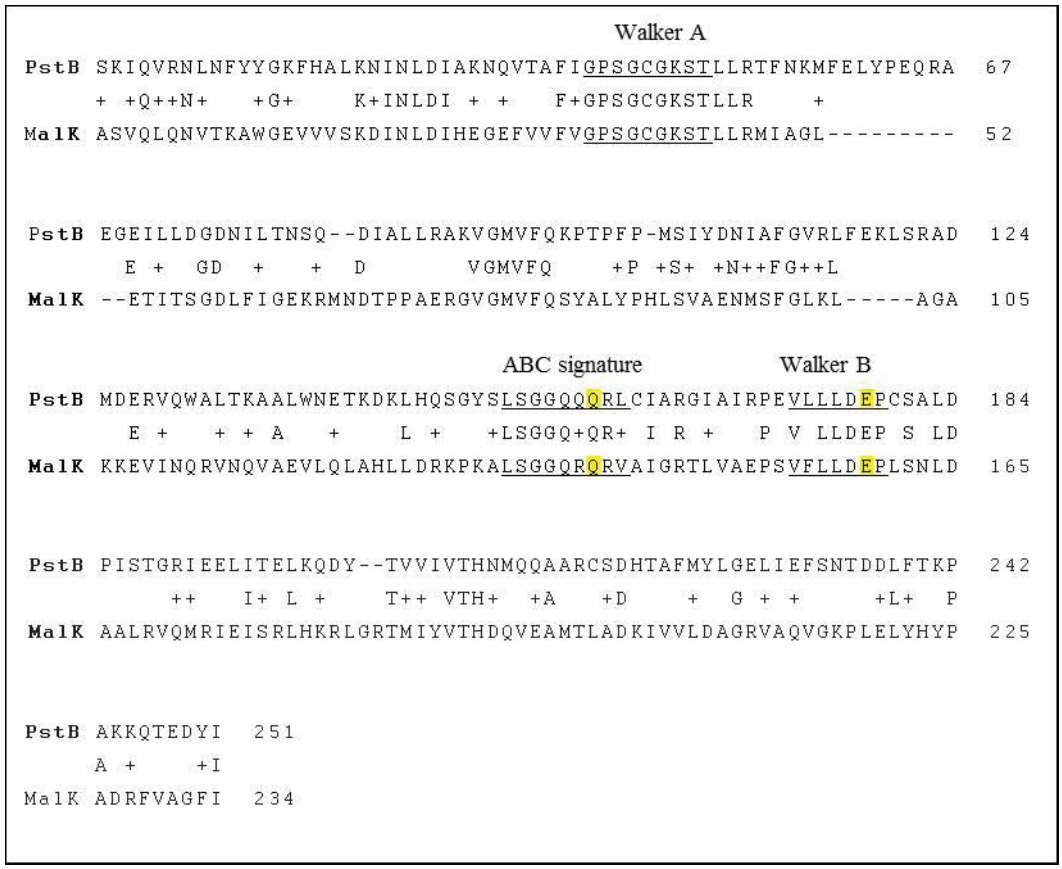

Figure 20: BLAST alignment of PstB and MalK

Alignment of protein sequences PstB and MalK, along with their corresponding mutations. The underlined amino acids represent three key motifs found in PstB. Labels for each motif are found above the underlined sequences. The residues selected for mutation are highlighted in yellow. The Q160K mutation in PstB switched a neutrally-charged glutamic acid, located in the Walker B motif, to a positively-charged lysine. The E179Q mutation traded a negatively-charged glutamine, located in the ABC signature motif, to a neutrally-charged glutamic acid.

Determine functionality of PstB mutants

Protein functionality, this time for the newly-created mutant strains, was once again established prior to co-purification or two-hybrid analyses. Mutant strains containing p48-*pstB*-E179Q-His or p48-*pstB*-Q160-His plasmids were studied for functionality by performing alkaline phosphatase assays. For cultures grown in MOPS high phosphate medium, the mutant

strain containing p48-*pstB*-E179Q-His exhibited high levels of alkaline phosphatase similar to the Δ*pstB* strain with pRR48 (negative control), demonstrating that the E179Q mutant is unable to signal (see Fig. 21). These results also demonstrate that the E179Q mutation overrides the His-tag effects of constitutive phosphate signaling. Conversely, the mutant strain containing p48-*pstB*-Q160K-His produced low levels of alkaline phosphatase in phosphate rich media, indicating active signaling capabilities (Fig. 21). In MOPS low phosphate media, the *pstB*-E179Q-His mutant again produced high alkaline phosphatase levels close to that of the negative control, while the *pstB*-Q160K-His mutant produced activity levels closer to the wild type positive control (see Fig. 22).

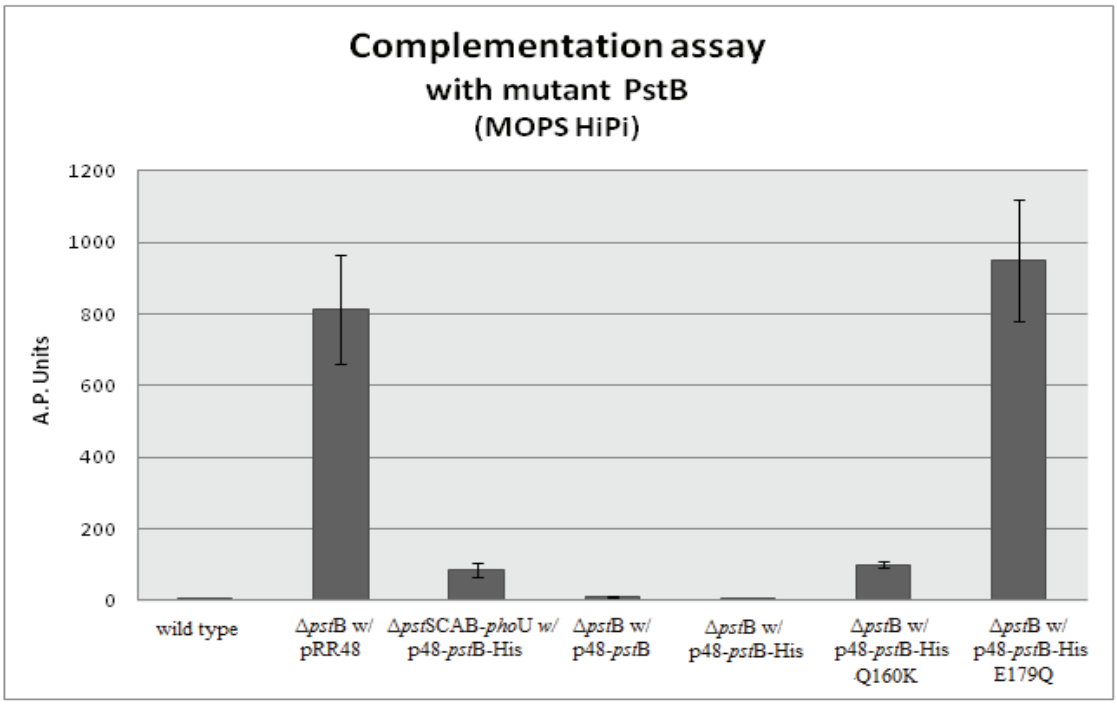

Figure 21: Alkaline phosphatase assay comparing mutant strains (MOPS HiP_i)

Alkaline phosphatase assays were performed on the following strains grown in 1 X MOPS high phosphate medium: wild type, a Δ*pstB* strain with pRR48, a Δ*pstSCAB-phoU* strain with p48-*pstB*-His, a Δ*pst* strain with p48-*pstB,* a Δ*pstB* strain with p48-*pstB*-His, a Δ*pstB* strain with p48-*pstB*-Q160K-His, and a Δ*pstB* strain with p48-*pstB*-E179Q-His. Error bars measure standard deviations for triplicate samples.

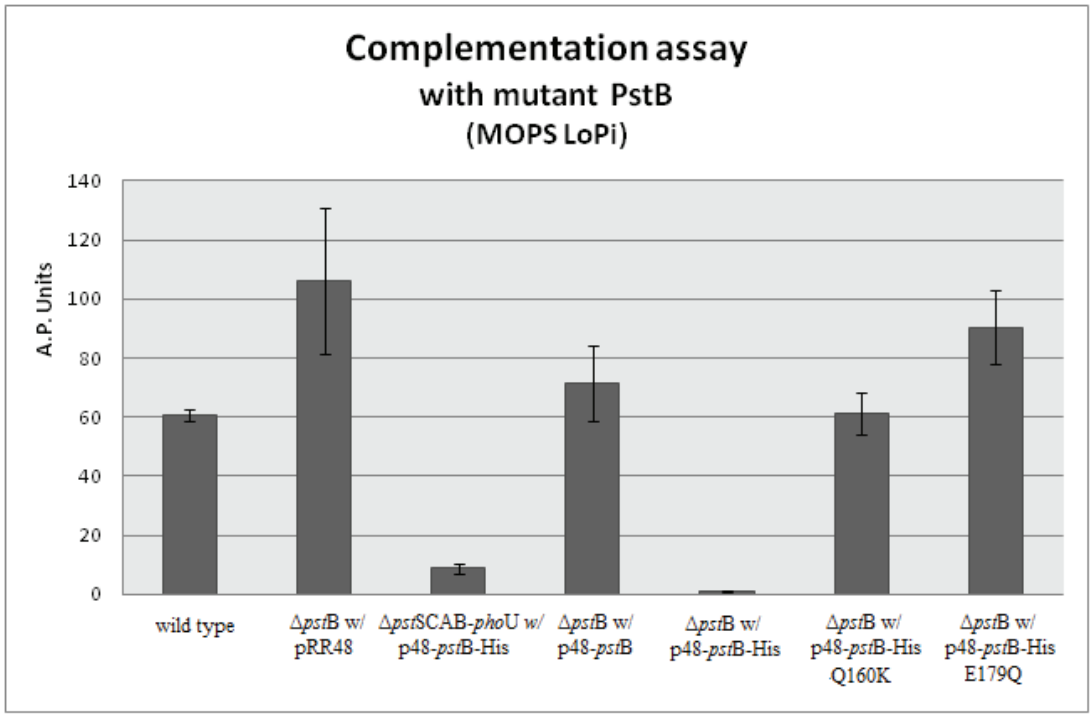

Figure 22: Alkaline phosphatase assay comparing mutant strains (MOPS LoP$_i$)

Alkaline phosphatase assays were performed on the following strains grown in 1 X MOPS high phosphate medium: wild type, a Δ*pstB* strain with pRR48, a Δ*pstSCAB-phoU* strain with p48-*pstB*-His, a Δ*pst* strain with p48-*pstB,* a Δ*pstB* strain with p48-*pstB*-His, a Δ*pstB* strain with p48-*pstB*-Q160K-His, and a Δ*pstB* strain with p48-*pstB*-E179Q-His. Error bars measure standard deviations for triplicate samples.

Mutant PstB-PhoU interactions observed via co-purification and co-immunoblotting

Once protein functionality for the mutant strains was determined, the next goal was to establish if mutations made to PstB altered its interactions with PhoU. To study these interactions, mutant versions of PstB-His (E179Q and Q160K) were co-purified on a Hi-Trap nickel sepharose column and immunoblotted with mouse polyclonal α-His antibody and rabbit polyclonal α-PhoU antibody, as described in Materials and Methods.

As seen in Fig. 23, PhoU was shown to co-elute in the same fractions as mutant E179Q PstB-His and mutant Q160K PstB-His. These results demonstrate that regardless of mutant conformations, PstB and PhoU still interact.

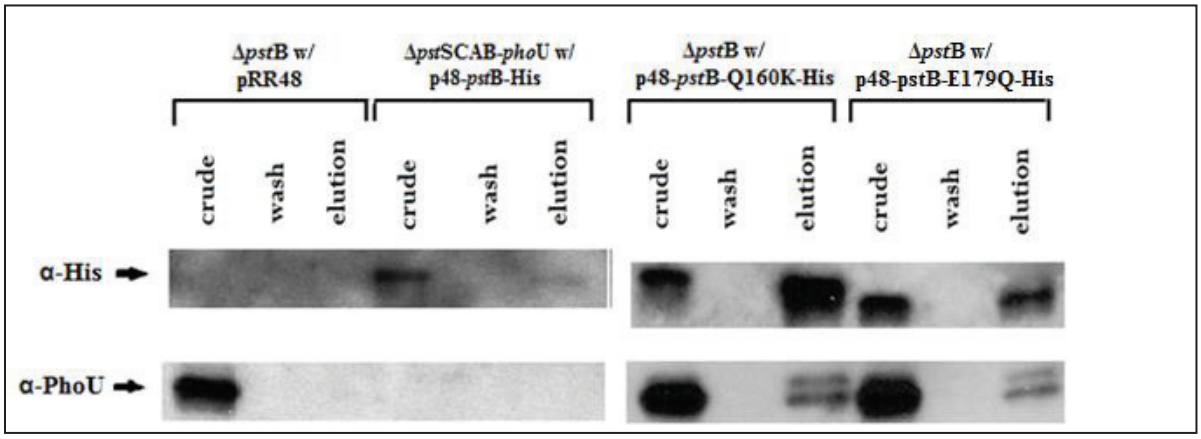

Figure 23. Western blot testing "locked" mutant PstB interactions with PhoU

Control strains, a Δ*pstB* strain with pRR48 and a Δ*pstSCAB-phoU* strain with p48-*pstB*-His, and test strains, a Δ*pstB* strain with p48-*pstB*-Q160K-His and a Δ*pstB* strain with p48-*pstB*-E179Q-His, were cultured in MOPS low phosphate medium. Lysed cells were co-purified and protein from selected fractions of each sample as separated with SDS-PAGE. Protein was separately probed with with α-His and α-PhoU antibodies.

Mutant PstB-PhoU interactions verified through two-hybrid screening

Though the E179Q and Q160K mutations made to PstB are assumed to affect conformational changes in the entire transporter complex, an understanding of how PhoU interacts with mutant versions of PstB alone could still shed light on how their interactions when PstB is functioning within the entire transporter complex. To study this, we used the bacterial adenylate cyclase two-hybrid system to analyze protein-protein interactions between mutant PstB and PhoU.

Results from plating co-transformed strains on MacConkey/maltose plates showed dark red colonies for the pUT18C-*pstB* and pKT25-*phoU* strain and the zip positive control strains. Colonies from the strains containing pUT18C containing mutant Q160K *pstB* or mutant E179Q *pstB* and the pKT25-*phoU* exhibited a lighter red phenotype (see Fig. 24). However, the strain containing mutant E179Q *pstB* turned substantially darker than the strain containing mutant Q160K *pstB* after an additional 24 hr of incubation (Fig. 24). Negative control colonies all remained white. These results, once again, confirm a protein-protein interaction between wild type PstB and PhoU. Additionally, the light red phenotype may indicate a weaker interaction between mutant PstB (E179Q or Q160K) and PhoU, though mutant E179Q PstB appears to interact more tightly with PhoU than mutant Q160K PstB.

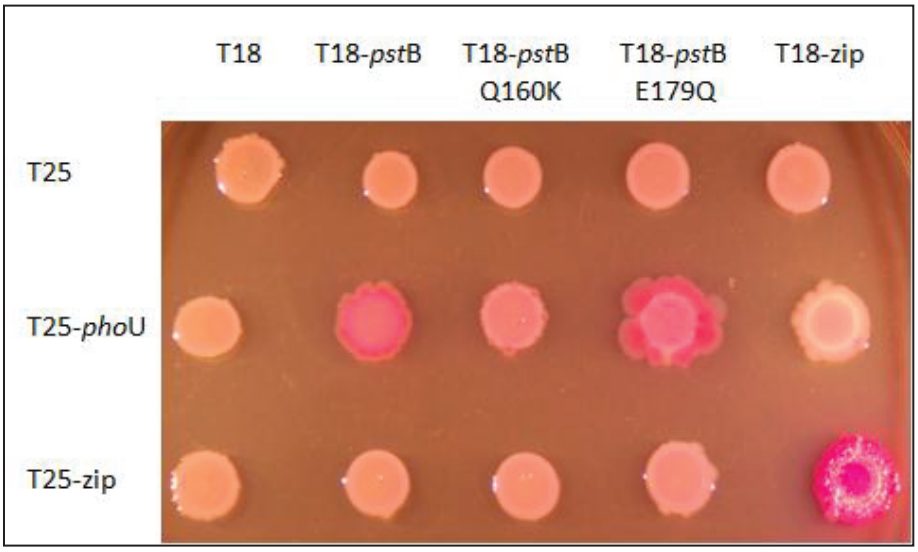

Figure 24. Two-hybrid analysis of "locked" PstB mutant interactions with PhoU

Test and control strains were spotted onto MacConkey/maltose plates and incubated for 36-48 hr. White colonies indicate no protein interactions taking place; deep red colonies indicate protein-protein interactions.

Aim 3: Determine if transport of P_i induces signal transduction

To address the issue of whether signal transduction is triggered by imported inorganic phosphate (P_i) or the conformational changes in the PstSCAB$_2$ transporter, a phosphate transport assay was performed. This assay was used to determine whether the two mutant PstSCAB$_2$ transporters, as well as the reconstituted wild type transporter, maintained their phosphate transport function. These strains were compared to a wild type strain and a Δ*pstSCAB-phoU* strain as positive and negative controls, respectively. Since signaling capabilities for each strain were previously established with alkaline phosphatase assays, being able to determine if signaling could occur independently of phosphate transport would provide a mechanistic distinction in how this process takes place. If the transporter, locked in a signaling conformation (Q160K), is able to signal even when phosphate transport is inhibited, it can be concluded that inorganic phosphate transport is not the mechanism by which signal transduction is transmitted.

Phosphate transport assays measuring uptake of radioactively labeled inorganic phosphate ($^{32}P_i$) were used to determine if strains reconstituted with wild type *pstB*, E179Q mutant *pstB*, and Q160K mutant *pstB* were functional for phosphate transport (see Fig. 10 for experiment overview). As seen in Fig. 25, the Δ*pstB* strain with p48-*pstB* strain was capable of transporting $^{32}P_i$ at a high rate, as was the wild type positive control. However, both mutant strains as well as the the Δ*pstSCAB-phoU* negative control showed negligible $^{32}P_i$ uptake. These results indicate that signal transduction can still occur, regardless of the transporter's ability to transport phosphate into the cell.

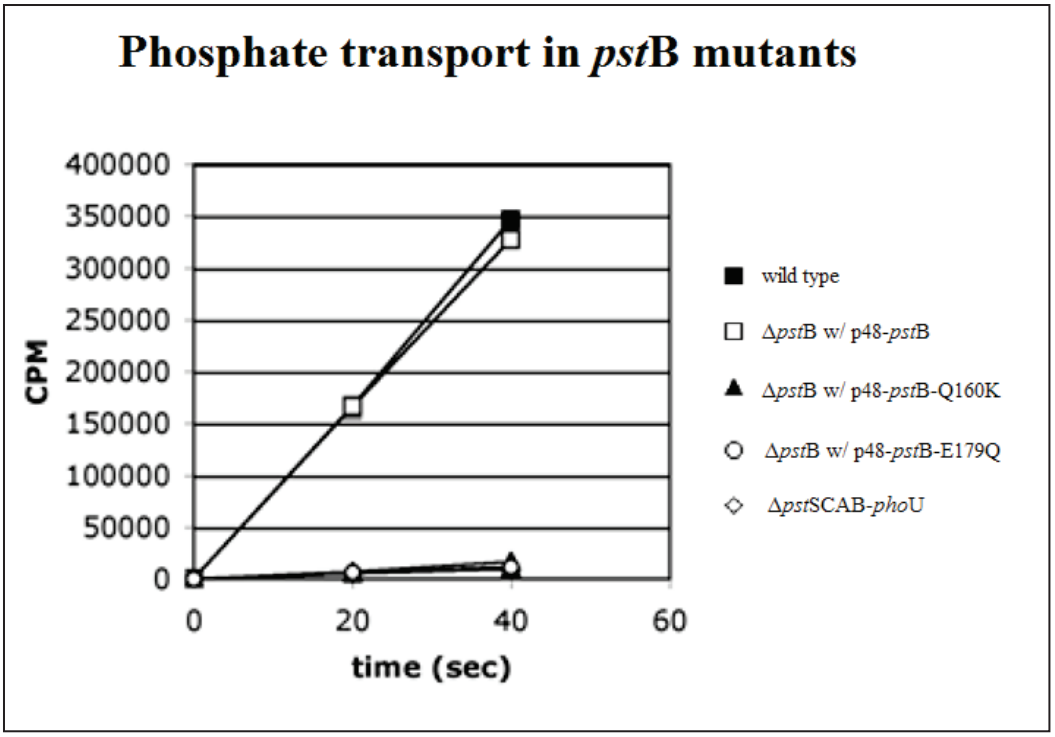

Figure 25. Phosphate transport assay

Phosphate transport assays were performed on the following: wild type, a Δ*pstB* strain with p48*pstB*, a Δ*pstB* strain with p48*pstB*-Q160K, a Δ*pstB* strain with p48*pstB*-E179Q, and a Δ*pstSCAB-phoU* strain. The wild type strain and the Δ*pstSCAB-phoU* strain were used as positive and negative controls, respectively.

DISCUSSION

When the surrounding environment has abundant phosphate, *Escherichia coli* will use as few resources as possible to facilitate its intake. However, when environmental phosphate levels are scarce, the cell will expend energy to upregulate expression of target genes used to acquire phosphate from alternate phosphorous sources. These genes comprise the Pho regulon, which is inhibited when phosphate levels are high, and activated when levels are low. Pho gene regulation is controlled by the TCS, PhoR-PhoB, which constitutively activates gene expression unless inhibited by an external signal. Since the histidine kinase, PhoR, has no periplasmic sensory domain, this signal must be received indirectly. Signal transduction for TCS inhibition is dependent on expression of $PstSCAB_2$, a phosphate ABC transporter, and PhoU, an accessory peripheral membrane protein. To this point, the protein-protein interaction of these seven proteins in phosphate signal transduction has remained ambiguous.

In a recent review of the Pho regulon, Hsieh and Wanner suggested a model proposing $PstSCAB_2$ as the sensory mechanism used to transmit the phosphate signal to PhoR (4). In this model, PhoU acts as an accessory protein that mediates the formation of a signaling complex between $PstSCAB_2$ and PhoR. Another model of the system suggests, instead, that PhoU acts as a soluble messenger for PhoR, requiring no complex formation for signaling to occur (78). However, none of the protein interactions proposed by these models have been previously demonstrated.

We propose that direct interaction between $PstSCAB_2$, PhoU and PhoR, in a signaling complex, is the process by which the phosphate signal is transduced. The purpose of our research was to answer three questions from this model: Are there direct protein-protein interactions taking place between PstB and PhoU? Do conformational changes in $PstSCAB_2$ affected PstB-

PhoU interactions? And is signal transduction induces by the transport of P_i or the conformational changes of $PstSCAB_2$?

Biochemical and genetic approaches were used to address these questions. The primary technique used to identify potential interactions between PstB and PhoU was nickel co-purification analyzed by Western immunoblotting. Co-purification is an effective procedure used to identify or verify protein-protein interactions. It is especially helpful when studying interactions of protein complexes, as it provides a method to purify these complexes in a native setting. For example, Daus *et al*. employed the use of nickel purification to isolate His-tagged $MalFGK_2$ in order to better characterize the transporter's conformations (59). The ability to purify complete, functional protein complexes is important, as proteins may interact differently in a complex than they do alone. By using nickel column co-purification we were able to identify protein-protein interactions between PhoU and PstB as part of the complete $PstSCAB_2$ transporter. This method of testing for PstB-PhoU interactions proved invaluable in demonstrating the interactions between PhoU and PstB in native and mutant forms of the $PstSCAB_2$ complex.

The bacterial adenylate cyclase two-hybrid (BACTH) system was a complementary technique used to verify results from our co-purification experiments. Extensive research done by Karimova and Ladant, have demonstrated that this specific bacterial two-hybrid system provides an effective method for testing potential protein-protein interactions, and is a useful alternative to the traditional yeast two-hybrid system (79-81). For our purposes, using the *E. coli* system provided a more natural, prokaryotic environment for studying the protein interactions of PstB and PhoU. The BACTH *E. coli* system also allows for greater plasmid transformation efficiency as well as faster growth rates. Additionally, this system provides a simpler setting to

study eukaryotic, as well as prokaryotic, interactions such as membrane-localized, cytosolic, or DNA-associated protein-protein interactions. Plasmids from this system can also be used to identify putative binding partners via library screening, as described in the BACTH System Kit handbook (EuroMedex). We used the bacterial adenlyate cyclase two-hybrid system to verify PstB-PhoU interactions. Protein interactions from our genetically engineered strains were analyzed qualitatively on MacConkey/maltose plates, and quantitatively with β-galactosidase assays. Though this system did not provide a method to test native interactions of PhoU with complexed PstB, it was still effective in verifying protein-protein interactions observed from co-purification experiments. For our purposes, this system was an effective confirmatory tool to verify PstB-PhoU interactions.

Once PstB-PhoU interactions were determined, our next focus was to establish the affect of $PstSCAB_2$ conformations on these protein-protein interactions. As part of its catalytic cycle, PstB alternates between two conformations as it hydrolyzes ATP. This ATPase activity provides the energy needed to open and close $PstSCAB_2$ to initiate transport of P_i into the cell. When environmental phosphate levels are high an active phosphate signal is initiated in order to halt the expression of Pho genes. Additionally, with high amounts of phosphate in the environment, the $PstSCAB_2$ transporter will primarily be in an open conformation as it actively pumps phosphate into the cell. On the other hand, when environmental phosphate is low the phosphate signal is inhibited inducing the expression of Pho genes. In these low phosphate conditions, $PstSCAB_2$ remains primarily closed as it waits for PstS to present bound phosphate. The correlation between signaling ability and $PstSCAB_2$ conformations indicate that phosphate signaling may be affected by the predominant conformation of $PstSCAB_2$ in certain

environmental conditions. In fact, we believe the open and closed conformations of $PstSCAB_2$ are the mechanism by which the histidine kinase, PhoR, senses external phosphate levels.

To study how these conformations might affect signal transduction, we introduced two separate mutations to $PstSCAB_2$ designed to "lock" the transporter in open and closed conformations. Rational for these mutants came from research performed by Daus *et al.* on the homolog transporter, $MalFGK_{2\ (59)}$. Mutations were introduced to key residues of the Walker B and ABC signature motifs of MalK to alter transporter conformations. By inhibiting the hydrolyzing ability of the Walker B motif, the transporter would lack the catalytic energy to open for substrate transport—"locking" it closed. Conversely, by hampering MalK's ability to interact and stabilize bound ATP in the sister dimer, the transporter would not close—"locking" it in an open conformation. After introducing similar mutations to PstB, we used co-purification and BACTH experiments to determine if "locked" conformations of $PstSCAB_2$ affected protein interactions between PstB and PhoU.

Results from co-purification and BACTH experiments indicated that PhoU maintained interactions with both PstB mutant conformations (Q160K and E179Q). While the mechanisms of signal transduction cannot be determined from these data, it can be concluded that PhoU remains interacting with the nucleotide-binding domain of $PstSCAB_2$ in both closed (E179Q) and open (Q160K) conformations. This interaction appears to be constant, though perhaps varies in strength. A model explaining these findings involves a chain affect of conformational changes between $PstSCAB_2$ and PhoU. As the ABC transporter alternates between open and closed conformations, it also alters the conformation of PstB causing it to reveal or conceal interactive sites that allow tighter or looser interactions with PhoU. The conformational changes in PstB

may, in turn, alter the conformation of PhoU either allowing it, or preventing it, from interacting with PhoR.

Data from the phosphate transport assay, along with results provided from previous alkaline phosphatase assays, further clarified the final question regarding mechanisms of phosphate signal transduction in *E. coli*. The uptake assay determined that regardless of the transporter's ability or inability to transport phosphate into the cell, phosphate signal transduction would still occur. Though the exact mechanism of signal transduction cannot be determined from the phosphate transport results, it can be concluded that transport with resultant changes in internal P_i concentrations is not how the signal is transduced.

With these insights, this paper offers a revised model of Pho regulon signal transduction that supports and clarifies the Hsieh and Wanner model (see Fig. 17) (4). This model proposes a direct interaction between PhoU and the PstB dimer of $PstSCAB_2$. As $PstSCAB_2$ alternates between open and closed states, PstB and PhoU maintain protein interactions, but undergo subsequent conformational changes. This chain of conformational changes, in turn, affects interactions between PhoU and PhoR. When $PstSCAB_2$ is active and open, it puts PhoU in a conformational state that cannot interact with PhoR, allowing PhoR to remain as a kinase and enact expression of Pho genes. Conversely, when $PstSCAB_2$ is in a closed, resting state, PhoU's conformation is altered in a manner that allows it to interact with PhoR, initiating the PhoR phosphatase function and, in turn, inhibiting expression.

A future experiment testing whether wild type PstB-His is capable of transporting phosphate into the cell would be of particular interest. Since PstB-His exhibits the unique characteristic of constitutively transducing the phosphate signal, regardless of environmental

phosphate levels, determining whether the His-tag prevents phosphate transport would provide added insight to the mechanisms involved in signal transduction. We also plan to employ co-purification and BACTH experiments, similar to those used in this study, to demonstrate potential protein-protein interactions between PhoU and PhoR, and PstB and PhoR. As we move forward in this research, we hope to continue to shed light and further clarify the mechanisms involved in signal transduction of the Pho regulon of *Escherichia coli*.

REFERENCES

1. **Rees DC, Johnson E, Lewinson O.** 2009. ABC transporters: the power to change. Nat Rev Mol Cell Biol **10:**218-227.

2. **Surin BP, Rosenberg H, Cox GB.** 1985. Phosphate-specific transport system of Escherichia coli: nucleotide sequence and gene-polypeptide relationships. Journal of bacteriology **161:**189-198.

3. **Crepin S, Chekabab SM, Le Bihan G, Bertrand N, Dozois CM, Harel J.** 2011. The Pho regulon and the pathogenesis of Escherichia coli. Veterinary microbiology **153:**82-88.

4. **Hsieh YJ, Wanner BL.** 2010. Global regulation by the seven-component Pi signaling system. Current opinion in microbiology **13:**198-203.

5. **Wanner BL.** 1996. Signal transduction in the control of phosphate-regulated genes of Escherichia coli. Kidney international **49:**964-967.

6. **Robinson VL, Buckler DR, Stock AM.** 2000. A tale of two components: a novel kinase and a regulatory switch. Nature structural biology **7:**626-633.

7. **Stock AM, Robinson VL, Goudreau PN.** 2000. Two-component signal transduction. Annual review of biochemistry **69:**183-215.

8. **Mascher T, Helmann JD, Unden G.** 2006. Stimulus perception in bacterial signal-transducing histidine kinases. Microbiology and molecular biology reviews : MMBR **70:**910-938.

9. **Galperin MY.** 2006. Structural classification of bacterial response regulators: diversity of output domains and domain combinations. J Bacteriol **188:**4169-4182.

10. **Moglich A, Ayers RA, Moffat K.** 2009. Structure and signaling mechanism of Per-ARNT-Sim domains. Structure **17:**1282-1294.

11. **Mascher T.** 2006. Intramembrane-sensing histidine kinases: a new family of cell envelope stress sensors in Firmicutes bacteria. FEMS microbiology letters **264:**133-144.

12. **Parkinson JS, Kofoid EC.** 1992. Communication modules in bacterial signaling proteins. Annual review of genetics **26:**71-112.

13. **Moglich A, Ayers RA, Moffat K.** 2009. Design and signaling mechanism of light-regulated histidine kinases. Journal of molecular biology **385:**1433-1444.

14. **Tanaka T, Saha SK, Tomomori C, Ishima R, Liu DJ, Tong KI, Park H, Dutta R, Qin L, Swindells MB, Yamazaki T, Ono AM, Kainosho M, Inouye M, Ikura M.** 1998. NMR structure of the histidine kinase domain of the E-coli osmosensor EnvZ. Nature **396:**88-92.

15. **Auesukaree C, Homma T, Tochio H, Shirakawa M, Kaneko Y, Harashima S.** 2004. Intracellular phosphate serves as a signal for the regulation of the PHO pathway in Saccharomyces cerevisiae. The Journal of biological chemistry **279:**17289-17294.

16. **Stock J.** 1999. Signal transduction: Gyrating protein kinases. Curr Biol **9:**R364-R367.

17. **Igo MM, Ninfa AJ, Stock JB, Silhavy TJ.** 1989. Phosphorylation and dephosphorylation of a bacterial transcriptional activator by a transmembrane receptor. Genes & development **3:**1725-1734.

18. **Bilwes AM, Alex LA, Crane BR, Simon MI.** 1999. Structure of CheA, a signal-transducing histidine kinase. Cell **96:**131-141.

19. **Tomomori C, Tanaka T, Dutta R, Park H, Saha SK, Zhu Y, Ishima R, Liu D, Tong KI, Kurokawa H, Qian H, Inouye M, Ikura M.** 1999. Solution structure of the homodimeric core domain of Escherichia coli histidine kinase EnvZ. Nature structural biology **6:**729-734.

20. **Keener J, Kustu S.** 1988. Protein-Kinase and Phosphoprotein Phosphatase-Activities of Nitrogen Regulatory Proteins Ntrb and Ntrc of Enteric Bacteria - Roles of the Conserved Amino-Terminal Domain of Ntrc. Proceedings of the National Academy of Sciences of the United States of America **85:**4976-4980.

21. **Grebe TW, Stock JB.** 1999. The histidine protein kinase superfamily. Adv Microb Physiol **41:**139-227.

22. **Gao R, Mack TR, Stock AM.** 2007. Bacterial response regulators: versatile regulatory strategies from common domains. Trends in biochemical sciences **32:**225-234.

23. **Galperin MY.** 2006. Structural classification of bacterial response regulators: diversity of output domains and domain combinations. Journal of bacteriology **188:**4169-4182.

24. **West AH, Stock AM.** 2001. Histidine kinases and response regulator proteins in two-component signaling systems. Trends in biochemical sciences **26:**369-376.

25. **Barbieri CM, Wu T, Stock AM.** 2013. Comprehensive Analysis of OmpR Phosphorylation, Dimerization, and DNA Binding Supports a Canonical Model for Activation. Journal of molecular biology.

26. **Lukat GS, McCleary WR, Stock AM, Stock JB.** 1992. Phosphorylation of bacterial response regulator proteins by low molecular weight phospho-donors. Proceedings of the National Academy of Sciences of the United States of America **89:**718-722.

27. **Stock AM, Martinez-Hackert E, Rasmussen BF, West AH, Stock JB, Ringe D, Petsko GA.** 1993. Structure of the Mg(2+)-bound form of CheY and mechanism of phosphoryl transfer in bacterial chemotaxis. Biochemistry **32:**13375-13380.

28. **Birck C, Mourey L, Gouet P, Fabry B, Schumacher J, Rousseau P, Kahn D, Samama JP.** 1999. Conformational changes induced by phosphorylation of the FixJ receiver domain. Structure **7:**1505-1515.

29. **Halkides CJ, McEvoy MM, Casper E, Matsumura P, Volz K, Dahlquist FW.** 2000. The 1.9 A resolution crystal structure of phosphono-CheY, an analogue of the active form of the response regulator, CheY. Biochemistry **39:**5280-5286.

30. **Kern D, Volkman BF, Luginbuhl P, Nohaile MJ, Kustu S, Wemmer DE.** 1999. Structure of a transiently phosphorylated switch in bacterial signal transduction. Nature **402:**894-898.

31. **Lee SY, Cho HS, Pelton JG, Yan D, Henderson RK, King DS, Huang L, Kustu S, Berry EA, Wemmer DE.** 2001. Crystal structure of an activated response regulator bound to its target. Nature structural biology **8:**52-56.

32. **Lewis RJ, Brannigan JA, Muchova K, Barak I, Wilkinson AJ.** 1999. Phosphorylated aspartate in the structure of a response regulator protein. Journal of molecular biology **294:**9-15.

33. **Mack TR, Gao R, Stock AM.** 2009. Probing the roles of the two different dimers mediated by the receiver domain of the response regulator PhoB. Journal of molecular biology **389:**349-364.

34. **Matsushika A, Mizuno T.** 1998. A dual-signaling mechanism mediated by the ArcB hybrid sensor kinase containing the histidine-containing phosphotransfer domain in Escherichia coli. Journal of bacteriology **180:**3973-3977.

35. **Ulrich LE, Zhulin IB.** 2007. MiST: a microbial signal transduction database. Nucleic acids research **35:**D386-390.

36. **De Carlo S, Chen B, Hoover TR, Kondrashkina E, Nogales E, Nixon BT.** 2006. The structural basis for regulated assembly and function of the transcriptional activator NtrC. Genes & development **20:**1485-1495.

37. **Toro-Roman A, Wu T, Stock AM.** 2005. A common dimerization interface in bacterial response regulators KdpE and TorR. Protein science : a publication of the Protein Society **14:**3077-3088.

38. **Bachhawat P, Swapna GV, Montelione GT, Stock AM.** 2005. Mechanism of activation for transcription factor PhoB suggested by different modes of dimerization in the inactive and active states. Structure **13:**1353-1363.

39. **Wanner BL.** 1992. Is cross regulation by phosphorylation of two-component response regulator proteins important in bacteria? Journal of bacteriology **174:**2053-2058.

40. **Wanner B.** 1996. Phosphorous assimilation and control of the phosphate regulon.

41. **Higgins CF, Hyde SC, Mimmack MM, Gileadi U, Gill DR, Gallagher MP.** 1990. Binding protein-dependent transport systems. Journal of bioenergetics and biomembranes **22:**571-592.

42. **Davidson AL, Maloney PC.** 2007. ABC transporters: how small machines do a big job. Trends in microbiology **15:**448-455.

43. **Dean M, Hamon Y, Chimini G.** 2001. The human ATP-binding cassette (ABC) transporter superfamily. Journal of lipid research **42:**1007-1017.

44. **Konings WN, Poelarends GJ.** 2002. Bacterial multidrug resistance mediated by a homologue of the human multidrug transporter P-glycoprotein. IUBMB life **53:**213-218.

45. **Efferth T.** 2001. The human ATP-binding cassette transporter genes: from the bench to the bedside. Current molecular medicine **1:**45-65.

46. **Higgins CF.** 2001. ABC transporters: physiology, structure and mechanism--an overview. Research in microbiology **152:**205-210.

47. **Dassa E, Schneider E.** 2001. The rise of a protein family: ATP-binding cassette systems. Research in microbiology **152:**203.

48. **Jones PM, George AM.** 2004. The ABC transporter structure and mechanism: perspectives on recent research. Cellular and molecular life sciences : CMLS **61:**682-699.

49. **Schmitt L, Tampe R.** 2002. Structure and mechanism of ABC transporters. Current opinion in structural biology **12:**754-760.

50. **Chen J, Sharma S, Quiocho FA, Davidson AL.** 2001. Trapping the transition state of an ATP-binding cassette transporter: evidence for a concerted mechanism of maltose transport. Proceedings of the National Academy of Sciences of the United States of America **98:**1525-1530.

51. **Moody JE, Millen L, Binns D, Hunt JF, Thomas PJ.** 2002. Cooperative, ATP-dependent association of the nucleotide binding cassettes during the catalytic cycle of ATP-binding cassette transporters. The Journal of biological chemistry **277:**21111-21114.

52. **Schneider E, Hunke S.** 1998. ATP-binding-cassette (ABC) transport systems: functional and structural aspects of the ATP-hydrolyzing subunits/domains. FEMS microbiology reviews **22:**1-20.

53. **Kranitz L, Benabdelhak H, Horn C, Blight MA, Holland IB, Schmitt L.** 2002. Crystallization and preliminary X-ray analysis of the ATP-binding domain of the ABC transporter haemolysin B from Escherichia coli. Acta crystallographica. Section D, Biological crystallography **58:**539-541.

54. **Zaitseva J, Jenewein S, Oswald C, Jumpertz T, Holland IB, Schmitt L.** 2005. A molecular understanding of the catalytic cycle of the nucleotide-binding domain of the ABC transporter HlyB. Biochemical Society transactions **33:**990-995.

55. **Davidson AL, Chen J.** 2004. ATP-binding cassette transporters in bacteria. Annual review of biochemistry **73:**241-268.

56. **Daus ML, Landmesser H, Schlosser A, Muller P, Herrmann A, Schneider E.** 2006. ATP induces conformational changes of periplasmic loop regions of the maltose ATP-binding cassette transporter. The Journal of biological chemistry **281:**3856-3865.

57. **Chen J, Lu G, Lin J, Davidson AL, Quiocho FA.** 2003. A tweezers-like motion of the ATP-binding cassette dimer in an ABC transport cycle. Molecular cell **12:**651-661.

58. **Austermuhle MI, Hall JA, Klug CS, Davidson AL.** 2004. Maltose-binding protein is open in the catalytic transition state for ATP hydrolysis during maltose transport. The Journal of biological chemistry **279:**28243-28250.

59. **Daus ML, Grote M, Muller P, Doebber M, Herrmann A, Steinhoff HJ, Dassa E, Schneider E.** 2007. ATP-driven MalK dimer closure and reopening and conformational changes of the "EAA" motifs are crucial for function of the maltose ATP-binding cassette transporter (MalFGK2). The Journal of biological chemistry **282:**22387-22396.

60. **Van Dien SJ, Keasling JD.** 1998. A dynamic model of the Escherichia coli phosphate-starvation response. J Theor Biol **190:**37-49.

61. **Surin BP, Dixon NE, Rosenberg H.** 1986. Purification of the phoU protein, a negative regulator of the pho regulon of Escherichia coli K-12. Journal of bacteriology **168:**631-635.

62. **Lamarche MG, Wanner BL, Crepin S, Harel J.** 2008. The phosphate regulon and bacterial virulence: a regulatory network connecting phosphate homeostasis and pathogenesis. FEMS microbiology reviews **32:**461-473.

63. **Wanner BL, Metcalf WW.** 1992. Molecular genetic studies of a 10.9-kb operon in Escherichia coli for phosphonate uptake and biodegradation. FEMS microbiology letters **79:**133-139.

64. **Harris RM, Webb DC, Howitt SM, Cox GB.** 2001. Characterization of PitA and PitB from Escherichia coli. Journal of bacteriology **183:**5008-5014.

65. **Wanner BL.** 1993. Gene regulation by phosphate in enteric bacteria. Journal of cellular biochemistry **51:**47-54.

66. **Wanner BL, Chang BD.** 1987. The phoBR operon in Escherichia coli K-12. Journal of bacteriology **169:**5569-5574.

67. **Blanco AG, Sola M, Gomis-Ruth FX, Coll M.** 2002. Tandem DNA recognition by PhoB, a two-component signal transduction transcriptional activator. Structure **10:**701-713.

68. **Kim SK, Kimura S, Shinagawa H, Nakata A, Lee KS, Wanner BL, Makino K.** 2000. Dual transcriptional regulation of the Escherichia coli phosphate-starvation-inducible psiE gene of the phosphate regulon by PhoB and the cyclic AMP (cAMP)-cAMP receptor protein complex. Journal of bacteriology **182:**5596-5599.

69. **Jiang W, Metcalf WW, Lee KS, Wanner BL.** 1995. Molecular cloning, mapping, and regulation of Pho regulon genes for phosphonate breakdown by the phosphonatase pathway of Salmonella typhimurium LT2. Journal of bacteriology **177:**6411-6421.

70. **Arribas-Bosacoma R, Kim SK, Ferrer-Orta C, Blanco AG, Pereira PJ, Gomis-Ruth FX, Wanner BL, Coll M, Sola M.** 2007. The X-ray crystal structures of two

constitutively active mutants of the Escherichia coli PhoB receiver domain give insights into activation. Journal of molecular biology **366:**626-641.

71. **Ashenberg O, Keating AE, Laub MT.** 2013. Helix Bundle Loops Determine Whether Histidine Kinases Autophosphorylate in cis or in trans. Journal of molecular biology.

72. **Lu G, Westbrooks JM, Davidson AL, Chen J.** 2005. ATP hydrolysis is required to reset the ATP-binding cassette dimer into the resting-state conformation. Proceedings of the National Academy of Sciences of the United States of America **102:**17969-17974.

73. **Smith PC, Karpowich N, Millen L, Moody JE, Rosen J, Thomas PJ, Hunt JF.** 2002. ATP binding to the motor domain from an ABC transporter drives formation of a nucleotide sandwich dimer. Molecular cell **10:**139-149.

74. **Oganesyan V, Oganesyan N, Adams PD, Jancarik J, Yokota HA, Kim R, Kim SH.** 2005. Crystal structure of the "PhoU-like" phosphate uptake regulator from Aquifex aeolicus. Journal of bacteriology **187:**4238-4244.

75. **Hoffer SM, Tommassen J.** 2001. The phosphate-binding protein of Escherichia coli is not essential for P(i)-regulated expression of the pho regulon. Journal of bacteriology **183:**5768-5771.

76. **Neidhardt FC, Bloch PL, Smith DF.** 1974. Culture medium for enterobacteria. Journal of bacteriology **119:**736-747.

77. **Ames P, Studdert CA, Reiser RH, Parkinson JS.** 2002. Collaborative signaling by mixed chemoreceptor teams in Escherichia coli. Proceedings of the National Academy of Sciences of the United States of America **99:**7060-7065.

78. **Hoffer SM, Tommassen J.** 2001. The phosphate-binding protein of Escherichia coli is not essential for P(i)-regulated expression of the pho regulon. J Bacteriol **183:**5768-5771.

79. **Battesti A, Bouveret E.** 2012. The bacterial two-hybrid system based on adenylate cyclase reconstitution in Escherichia coli. Methods **58:**325-334.

80. **Karimova G, Ladant D, Ullmann A.** 2002. Two-hybrid systems and their usage in infection biology. International journal of medical microbiology : IJMM **292:**17-25.

81. **Karimova G, Ullmann A, Ladant D.** 2000. A bacterial two-hybrid system that exploits a cAMP signaling cascade in Escherichia coli. Methods in enzymology **328:**59-73.